







## Article

# Bacterioplankton Community Diversity of a Portuguese Aquifer System (Maciço Calcário Estremenho)

Daniela R. de Figueiredo <sup>1,\*</sup> , Maria T. Condesso de Melo <sup>2</sup> , Pedro P. Saraiva <sup>1</sup> , Joana Oliveira <sup>2</sup>, Ana M. M. Gonçalves <sup>3</sup> , Ana Sofia P. S. Reboleira <sup>4,5</sup> , Ana R. M. Polónia <sup>1</sup> , Nelson Abrantes <sup>1,\*</sup>  and Daniel F. R. Cleary <sup>1</sup> 

- <sup>1</sup> Department of Biology & CESAM (Centre for Environmental and Marine Studies), University of Aveiro, Campus Universitário de Santiago, 3810-193 Aveiro, Portugal; pedromsaraiva@ua.pt (P.P.S.); ritapolonia@ua.pt (A.R.M.P.); cleary@ua.pt (D.F.R.C.)
  - <sup>2</sup> Civil Engineering Research and Innovation for Sustainability (CERIS), Instituto Superior Técnico, Departamento de Engenharia de Recursos Minerais e Energéticos, Universidade de Lisboa, Av. Rovisco Pais, 1, 1049-001 Lisbon, Portugal; teresa.melo@tecnico.ulisboa.pt (M.T.C.d.M.); joana.s.oliveira@ist.utl.pt (J.O.)
  - <sup>3</sup> CFE—Centre for Functional Ecology: Science for People & Planet, Department of Life Sciences, University of Coimbra, 3000-456 Coimbra, Portugal; amgoncalves@uc.pt
  - <sup>4</sup> Centre for Ecology, Evolution and Environmental Changes (cE3c) & CHANGE-Global Change and Sustainability Institute, and Departamento de Biologia Animal, Faculdade de Ciências, Universidade de Lisboa, Campo Grande, 1749-016 Lisbon, Portugal; asreboleira@ciencias.ulisboa.pt
  - <sup>5</sup> Museu Nacional de História Natural e da Ciência, Universidade de Lisboa, Rua da Escola Politécnica, 1250-102 Lisbon, Portugal
- \* Correspondence: dfigueiredo@ua.pt (D.R.d.F.); njabrantes@ua.pt (N.A.)

**Abstract:** Climate change may increase the vulnerability of aquifers to contamination through extreme precipitation and extended drought periods. Therefore, the understanding of groundwater ecosystem dynamics is crucial, with bacterial assemblages playing a major role in biogeochemical cycles. The present research describes a geospatial study targeting the bacterial community structure of groundwaters from the largest karst aquifer in Portugal (the Maciço Calcário Estremenho), integrating hydrogeochemical and bacterial diversity data. A total of 22 samples were analyzed from a set of 11 geographically sparsely distributed groundwater sources in dry vs. wet seasons. The 16S rRNA gene barcoding data revealed bacterial community variability across samples in space and time. The phylum Proteobacteria was dominant across all samples (from 44 to 92% of total sequence reads), mainly represented by the classes Alphaproteobacteria (orders Sphingomonadales, BD7–3, Rhizobiales and Rhodospirillales), Betaproteobacteria (orders Burkholderiales, Rhodocyclales, Nitrosomonadales), Gammaproteobacteria (orders Pseudomonadales, Xanthomonadales, Alteromonadales, Legionellales) and Deltaproteobacteria (orders Myxococcales, Spirobaecillales). Variation in the bacterial community was primarily attributed to parameters such as redox conditions (DO, ORP), Fe, Mn, SO<sub>4</sub>, PO<sub>4</sub>, Sr and Cl, but also some minor and trace elements (Al, V, Cr, Cu, Pb). Our results provide novel insights into bacterial diversity in relation to groundwater hydrogeochemistry. The strong dominance of OTUs related to bacterial taxa associated with nitrification/denitrification also highlights a potentially important role of these assemblages on nutrients (nitrogen sources) and groundwater quality dynamics at this karstic aquifer system. Moreover, the integration of bacterial assemblages information is emphasized as central for water quality monitoring programs.

**Keywords:** groundwater quality; Maciço Calcário Estremenho; bacterial diversity; 16S rRNA gene metabarcoding



**Citation:** de Figueiredo, D.R.; Condesso de Melo, M.T.; Saraiva, P.P.; Oliveira, J.; Gonçalves, A.M.M.; Reboleira, A.S.P.S.; Polónia, A.R.M.; Abrantes, N.; Cleary, D.F.R. Bacterioplankton Community Diversity of a Portuguese Aquifer System (Maciço Calcário Estremenho). *Water* **2024**, *16*, 1858. <https://doi.org/10.3390/w16131858>

Academic Editor: Alejandro Gonzalez-Martinez

Received: 24 May 2024  
Revised: 16 June 2024  
Accepted: 22 June 2024  
Published: 28 June 2024



**Copyright:** © 2024 by the authors. Licensee MDPI, Basel, Switzerland. This article is an open access article distributed under the terms and conditions of the Creative Commons Attribution (CC BY) license (<https://creativecommons.org/licenses/by/4.0/>).

## 1. Introduction

Predicted changes to the climate include extended periods of warmth and increasing drought events with potentially important impacts on aquatic ecosystems [1–8]. Groundwaters from karst aquifers are an important source for drinking water and ecosystems [9],

but their vulnerability to contamination is particularly high [10–15]. Moreover, there is increasing concern regarding additional impacts from climate change due to drought intensification and extreme precipitation events, which enhance the exposure of aquifers to surface contaminants and the risk of contamination [16–18]. Worldwide karst areas usually comprise complex subsurface drainage systems, including hydrological networks, fissures, and caves originating from the natural erosion of limestone and the dissolution of calcium carbonate, which make these environments prone to contamination from surface diffuse pollution sources such as agriculture, livestock production, industrial activity and wastewater effluents [19–21]. This vulnerability, combined with the trend to lower annual precipitation levels, which have been reported for Southern Europe in recent decades [22], can impact groundwater availability and quality [23,24]. In Southern Portugal, in particular, the effects of historical reduction on precipitation levels have been more severe, with impacts on groundwater recharge intensified by a high irrigation pressure [25,26]. All these changes affect the whole aquifer ecosystem.

Bacterial communities play a fundamental role in groundwater geochemical cycles [27,28], and their diversity and dynamics are thus also modulated by the hydro-geochemical conditions of the aquifer. Bacterial assemblages have been shown to remain stable in karst groundwater ecosystems [29], indicating that shifts in the bacterial community composition can provide potentially important information on the impact of pollution sources and fluctuations. Over the past two decades, the knowledge of the bacterial biodiversity from groundwater ecosystems has shown an impressive increase with recent culture-independent metagenomic approaches, namely DNA metabarcoding, providing new insights into the bacterial ecology of these environments [30–32]. However, for Portuguese groundwaters, the published information regarding the bacterial assemblages remains scarce [33–35]. Most information is based on culturing and/or the molecular detection of targeted pathogenic bacteria [36–42] or, if using culture-independent DNA-based techniques for community studies, only considering one or two groundwater sampling sites [33,35]. The present study aims to evaluate to what extent spatial and environmental data, including aquifer hydrogeochemistry, can explain variation in the bacterioplankton community of several springs and boreholes at the Maciço Calcário Estremenho (Central western Portugal). Therefore, this study is a strong contribution not only to the scarce knowledge concerning the bacterial community diversity in Portuguese groundwaters but also considering the ecological context. This is very important to create baseline information, particularly with the expected increase of extreme precipitation and drought episodes in the upcoming years. Moreover, it also explores the potential for the integration of whole bacterial community information through 16S rRNA gene metabarcoding as a promising tool for routine water quality assessment.

## 2. Materials and Methods

### 2.1. Study Area

Karst formations occupy a considerable area of the Portuguese territory [43,44]. The Maciço Calcário Estremenho-MCE (Estremenho Karst Massif) is located in Southwest Europe and Central Western region of Portugal (Figure 1A,B) and is an uplifted Jurassic limestone massif unit of the Lusitanian Basin hosting a very complex karst aquifer system, which is made up of several subsystems, each one related to a different perennial karst spring. The aquifer is formed by an extensive network of large and hydraulically connected Jurassic limestone caves, part of the Serras de Aire e Candeeiros Natural Park [45]. It is rich in geological resources [46] and also holds an important subterranean animal biodiversity [47]. The Maciço Calcário Estremenho aquifer is also an important contributor to the regional river base flow, with a large variety of groundwater-dependent ecosystems, and as a source of drinking water [45].

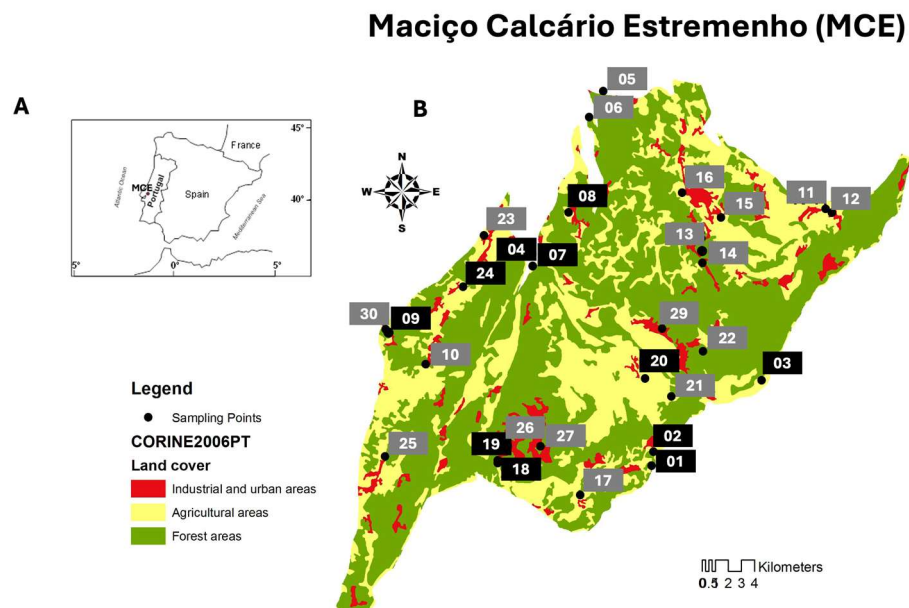


**Figure 1.** (A) Map of the location of the Maciço Calcário Estremenho (MCE) in Portugal and in the context of Southwestern Europe; (B) map of the sampling sites location at the MCE—the sites with samples used in the present study are highlighted in black boxes.

## 2.2. Sampling

Groundwater samples were collected from the discharge during pumping conditions once the stabilization of the principal field parameters—pH, water temperature (T), specific electrical conductance (SEC), reduction-oxidation potential (Eh) and dissolved oxygen (DO) under anaerobic conditions—was observed.

Samples collected for subsequent major, minor and trace element analyses were filtered in the field through MF-Millipore® 0.45 µm filter membranes (47 mm diameter, hydrophilic, and gridded; code HAWG04700). A 30 mL aliquot was acidified (1% *v/v* HNO<sub>3</sub> Aristar® grade), and a 60 mL aliquot was kept unacidified. All samples were sealed with parafilm, protected from sunlight, stored at 4 °C, and sent for laboratory analysis. For DNA extraction and analysis, approximately 5 L of groundwater samples were collected in 5L sterile bottles and immediately stored at 4 °C in the dark until further treatment at the laboratory on that same day.

A preliminary analysis of 30 groundwater sampling sites from the Maciço Calcário Estremenho was conducted for major, minor and trace element analyses, as well as for DNA extraction, from which only a total of 11 sites consisting of wells, and springs (Figure 1) were selected for full bacterial diversity characterization. Selection criteria were based on methodological requirements (e.g., field collection and sample processing protocols for DNA analyses). A total of 22 groundwater samples were then considered for the study, including two campaigns, in May 2012 and February 2013 (dry and wet seasons, respectively) (Table 1). The sampling campaigns lasted about one week for each period.

## 2.3. Quantification of Geochemical Parameters

Water temperature (T), specific electrical conductance (SEC), electrical conductivity (CE), reduction-oxidation potential (Eh), pH and dissolved oxygen (DO) were determined in situ using HANNA portable water testing meters and using a multiport flow-through cell connected in-line to the sampling points. On-site measurements also included the determination of alkalinity (quoted as HCO<sub>3</sub><sup>−</sup>) by acid titration using the standard colorimetric titration HACH® kit method.

**Table 1.** Groundwater sampling sites selected at the Maciço Calcário Estremenho (Portugal).

Sampling Site						Sample		
Site	Location	M (X)	P (Y)	Source Type	CODE	Sampling Date	Total Valid Sequences	Sampling Depth (m)
01	Nascente do Alviela	150043,00	275614.00	Spring	01F	27/02/2013	963	34
					01M	28/05/2012	1101	73
02	Ribeira dos Amiais	150166,02	276674.22	Waterline	02F	27/02/2013	1221	22
					02M	28/05/2012	1335	108
03	Nascente do Almonda	158424,00	282140.00	Spring	03F	27/02/2013	1505	12
					03M	28/05/2012	869	57
04	Nascente do Lena	140961,00	290852.00	Spring	04F	18/02/2013	1044	24
					04M	29/05/2012	1074	36
07	Poço da Ribeira do Lena	140969,26	290865.96	Well	07F	18/02/2013	1296	19
					07M	29/05/2012	1079	39
08	Fonte Alqueidão da Serra	143702,33	294962.89	Borehole	08F	18/02/2013	1218	15
					08M	29/05/2012	1781	15
09	Chiqueda	129725,28	286042.20	Borehole	09F	19/02/2013	1013	32
					09M	29/05/2012	979	186
18	Valverde - Alcanede	138293,22	275809.88	Borehole	18F	20/02/2013	1584	297
					18M	01/06/2012	939	233
19	Valverde - Alcanede	138286,06	276022.14	Borehole	19F	20/02/2013	1727	114
					19M	01/06/2012	1693	262
20	Serra de Sto António	149536,33	282273.46	Borehole	20F	20/02/2013	1154	250
					20M	01/06/2012	1514	250
24	Casais de Santa Teresa	135647,01	289282.98	Borehole	24F	19/02/2013	1441	220
					24M	04/06/2012	1992	220

From filtered samples, the acidified 30 mL aliquot was analyzed for major, minor and trace elements (including Mg, Ca, Na, K, Si, Fe, Sr, Li, Be, B, Al, Sc, Ti, V, Cr, Mn, Co, Ni, Cu, Zn, Ga, Ge, As, Se, Rb, Y, Zr, Nb, Mo, Ag, Cd, In, Sn, Sb, Te, Cs, Ba, La, Ce, Pr, Nd, Sm, Eu, Gd, Tb, Dy, Ho, Er, Tm, Yb, Lu, Hf, Ta, W, Hg, Tl, Pb, Bi, Th and U) using Agilent 7900 Inductively Coupled Plasma Mass Spectrometry (ICP-MS) analysis. The 60 mL unacidified aliquot was used for the determination of chloride ( $\text{Cl}^-$ ), total oxidized nitrogen ( $\text{NO}_3\text{-N}$ ), nitrite ( $\text{NO}_2^-$ ), bromide ( $\text{Br}^-$ ) and fluoride ( $\text{F}^-$ ) by Thermo Scientific Dionex ion chromatography (IC). The inorganic determinations were performed by certified (ISO/IEC 170125) Activation laboratories in Ontario (Canada). The electro-neutrality (E.N.) condition expressed was used as a quality control for all the determinations and ionic mass balances with closing errors between  $\pm 5\%$  considered to be acceptable.

#### 2.4. DNA Extraction and 16S rRNA Gene Metabarcoding

In each corresponding sampling day, approximately 2.5 L of groundwater samples were filtered through 0.22  $\mu\text{m}$  polycarbonate sterile filters and stored at  $-20^\circ\text{C}$ . Total DNA was extracted after resuspension in 2 mL of TE buffer [10 mM Tris HCl, 1 mM EDTA, pH 8.0] following centrifugation and a new resuspension in 200  $\mu\text{L}$  of TE buffer [48]. Lysis was carried out by adding lysozyme (1 mg  $\text{mL}^{-1}$ ) and incubating for 1 h at  $37^\circ\text{C}$ . DNA extraction and purification were performed using the Genomic DNA Purification Kit (MBI Fermentas, Vilnius, Lithuania), and DNA was resuspended in TE buffer and stored at  $-20^\circ\text{C}$ . Pyrosequencing libraries were obtained using the 454 Genome Sequencer FLX platform (Roche Diagnostics Ltd., West Sussex, UK). Bacterial 16S rRNA gene fragments from the V3V4 hypervariable region were amplified using barcoded fusion primers with the Roche-454 Titanium sequencing adapters A and B (an eight-base barcode sequence), the forward primer 5'-ACTCCTACGGGAGGCAG-3' (338F) and the reverse primer 5'-TACNVRGTHCTAATYC-3' (802R) [49,50]. PCR amplifications were carried out in 20  $\mu\text{L}$  reactions with Advantage Taq (Clontech) using 0.2 M of each primer, 0.2 mM dNTPs, 1 $\times$  of polymerase mix, 6% DMSO and 1–2  $\mu\text{L}$  of template DNA. PCR conditions were  $94^\circ\text{C}$  for 4 min, followed by 25 cycles of  $94^\circ\text{C}$  for 30 s,  $44^\circ\text{C}$  for 45 s and  $68^\circ\text{C}$  for 60 s and a final elongation step at  $68^\circ\text{C}$  for 10 min. Amplicons were quantified by fluorometry with PicoGreen (Invitrogen, Carlsbad, CA, USA), pooled at equimolar concentrations and sequenced in the A direction with GS 454 FLX Titanium chemistry, according to the manufacturer's instructions (Roche, 454 Life Sciences, Brandford, CT, USA),

at Biocant (Cantanhede, Portugal). Pyrosequencing sequence analysis was performed using previously described methods [51,52].

### 2.5. Sequence Analysis

Sequence analysis followed previously described methods [53,54]. Briefly, in QIIME, fasta and qual files were used as input for the `split_libraries.py` script. Operational Taxonomic Units (OTUs) were selected using UPARSE with `usearch7` [55]. Chimera checking was performed using the UCHIME algorithm [56]. OTU clustering was performed using the `-cluster_otus` command (cut-off threshold at 97%). Closely related organisms of numerically abundant OTUs ( $\geq 200$  sequences) were identified using the NCBI Basic Local Alignment Search Tool (BLAST) command line 'blastn' tool with the `-db` argument set to nt [57]. Bacterial 16S rDNA partial sequences generated in this study are available at NCBI SRA BioProject under the accession number PRJNA1009823.

### 2.6. Statistical Analysis

OTU, spatial and environmental matrices were imported into R [58]. Principal coordinate analysis (PCO) was used to explore the variation in the groundwaters among sampling sites. The environmental data were  $\log_e(x + 1)$  transformed, and the Bray–Curtis index was subsequently used followed by PCO. The Bray–Curtis similarity was chosen as opposed to the more frequently used Euclidean distance when dealing with this type of physico-chemical data because of the large number of values below the detection limit in the environmental data set. Spatial variation in the study area was modeled using principal coordinates of neighbor matrices (PCNMs). PCNM is a method for quantifying spatial trends across a range of scales and is based on the eigenvalue decomposition of a truncated matrix of geographic distances among sampling sites [59,60]. Significant PCNM eigenvectors were selected using the `pcnm` function in `Vegan` with 999 permutations. The OTU data matrix was  $\log_e(x + 1)$  transformed and further 'transformed' using the `decostand()` function in the `Vegan` package [61] in R. Through this transformation, the species abundance data were adjusted so that subsequent ordination analyses preserved the chosen distance among sample sites. In the present case, the Hellinger distance was used [62]. Then, two models were set up using redundancy analysis (RDA) with the Hellinger-transformed matrix as the response variable and spatial or environmental variables as explanatory variables. RDA arranges the data points in a multidimensional space where the axes represent gradients in species abundances, constrained by the explanatory variables (spatial and environmental variables) [63,64]. Here, the amount of variation in composition explained by the explanatory variables is the sum of all constrained eigenvalues divided by the total variation in the species data [64,65]. The spatial variables used here consisted of PCNM variables obtained using the `pcnm` function in `Vegan`. The environmental variables consisted of the first four PCO axes of the environmental data analysis and a dummy variable of sampling time in order to ascertain the impact of temporal variation and the concomitant difference in environmental parameters (e.g., temperature) on community composition. The `ordistep()` function was used in `Vegan` to select significant spatial and environmental predictors of variation in composition using backward selection, maximum permutations set to 1000, and a selection criterion of  $p = 0.10$ . The `rda()` function was used in R to perform the RDA and the `anova.cca()` function to test the significance of the RDA axes. Variance partitioning (with the `varpart` function in `Vegan`; [59,66]) was then used to partition the variance explained 1. purely by spatial variables (the purely spatial component); 2. purely by environmental variables (the purely environmental component); and 3. by a combination of spatial and environmental variables (the spatially structured environmental component). The significance of the RDA ordination axes was tested with the `anova()` function in `Vegan` with the 'by' argument set to 'axis'. This function tests the joint effect of constraints in RDA using an ANOVA like permutation test. Figures were generated in R software.



### 3. Results

#### 3.1. Environmental Parameters

The analysis of the environmental data set indicated significant differences in environmental conditions among sampling sites (see Figure 2). The main synthetic environmental gradient (PCO1: variance explained: 61%) separated sites (08, 18–20) with relatively high values of parameters such as Sr, SO<sub>4</sub> and PO<sub>4</sub> from remaining sites with relatively high values of OD1 (mg L), OD2 (%) and ORP. The second gradient (PCO2: variance explained: 12%) separated sites (08) with relatively high values of V and Cr from sites with relatively high values of Al (04 and 07 in February). The third axis (PCO3: variance explained: 11%) separated sites with relatively high values of Sr, PO<sub>4</sub>, V and Cr (07M, 18F, 04F and 08F) from sites with relatively high values of Cl, Cu, Pb, Mn and Zn (09M, 19M, 20M and 20F). The fourth axis (PCO4: variance explained: 10%) separated sites with relatively high values of Fe, Cs and SO<sub>4</sub> (18M and 07M) from sites with relatively high values of V (08F). The recorded environmental parameters showed marked variations across groundwater samples. Electrical conductivity (CE) varied between 397 and 2001 mS cm<sup>−1</sup>, at 04F and 18F, respectively, whereas pH varied between 6.6 (at 18M) and 7.49 (at 02M). Water temperature ranged from 15.90 to 20.54 °C (at 03F and 20F, respectively), depending on borehole depth. Samples from sites 01 and 02 had the highest dissolved oxygen concentrations (>10.00 mg L<sup>−1</sup>) in February. Sample 09M had the highest oxidation–reduction potential (ORP) (431.8 mV) and the highest concentration of Zn (56.3 mg L<sup>−1</sup>).

We also observed concentration peaks for certain parameters during February: the highest value for Ni was recorded at 01F (5.9 mg L<sup>−1</sup>), and a peak of Al was detected at 07F (59 mg L<sup>−1</sup>); Ba had a maximum of 56.8 mg L<sup>−1</sup> at sample 19F. The highest value for F (1.27 mg L<sup>−1</sup>) was recorded for sample 20M; sample 18F also had a high peak of Sr (9.70 mg L<sup>−1</sup>), followed by 19F (2.30 mg L<sup>−1</sup>); a peak concentration of PO<sub>4</sub> (0.93 mg L<sup>−1</sup>) was also recorded at 18F; at 20F, the highest concentration of Mn (7.1 mg L<sup>−1</sup>) was recorded. Interestingly, the concentrations of all these elements and ions were greatly reduced or undetectable in May, suggesting a strong probability of influence from surface effluent drainage into the aquifer. Nevertheless, sampling site 18 remained consistent for both February and May. Besides the highest values for conductivity (EC) (1896–2001 mS cm<sup>−1</sup>) and total dissolved solids (TDS) (949–1000 mg L<sup>−1</sup>), 18F and 18M also had the highest concentrations of Si (15.2–15.5 mg L<sup>−1</sup>), Fe (0.24–0.29 mg L<sup>−1</sup>), Sc (4 mg L<sup>−1</sup>), Ti (2.4–2.5 mg L<sup>−1</sup>), V (15.9–16.9 mg L<sup>−1</sup>), Li (16–19 mg L<sup>−1</sup>), B (55–56 mg L<sup>−1</sup>), Co (0.22–0.25 mg L<sup>−1</sup>), Rb (5.10–6.08 mg L<sup>−1</sup>), Cs (0.333–0.351 mg L<sup>−1</sup>) and Cr (1.0–1.8 mg L<sup>−1</sup>). Sample site 18 also had high concentrations of Ba (52.8–55.2 mg L<sup>−1</sup>). Site 20 also had, during both sampling campaigns, considerable concentrations of Zn (10.1–10.4 mg L<sup>−1</sup>) and Rb (5.60–5.98 mg L<sup>−1</sup>), as well as the highest values for HCO<sub>3</sub> (330–358 mg L<sup>−1</sup>), F (1.22–1.27 mg L<sup>−1</sup>), Cu (3.2–6.0 mg L<sup>−1</sup>), Mn (2.7–7.1 mg L<sup>−1</sup>), Pb (0.23–0.66 mg L<sup>−1</sup>) and U (1.24–1.28 mg L<sup>−1</sup>). These results highlight particular hydrogeological conditions of sampling sites 18 and 20 from deep boreholes (>300 m depth).

#### 3.2. 16S rRNA Gene Metabarcoding

The sequencing effort yielded 31,256 sequences, which were assigned to 5573 OTUs after quality control, OTU selection, and removal of chimeras, chloroplasts, mitochondria and sequences not assigned to the Bacteria domain. The most abundant phylum overall was Proteobacteria, which ranged from a total of 43.3% in 09M to 92.1% in 24M, with the most abundant classes including the Alpha-, Beta-, Gamma- and Deltaproteobacteria (Figure 3A). The phylum Nitrospirae was also dominant in some samples, reaching a maximum of 36.6% in 18M, followed by other locally abundant phyla such as Bacteroidetes (0.6 to 18.0%) and Actinobacteria (0.6 to 16.2%). Burkholderiales dominated the Betaproteobacteria in most samples (Figure 3B), except for samples from sites 18 and 20, which were mainly dominated by the orders Nitrosomadales and Rhodocyclales, respectively. For Alphaproteobacteria, Sphingomonadales also dominated the majority of samples (Figure 3C), except for 07M, 08M, 18F, 19M, 19F, 20M and 20F. In these samples, higher abundances for the orders BD7–3

and Rhodospirillales were recorded. Xanthomonadales and Legionellales were dominant orders of Gammaproteobacteria in most samples, except for sample 24M, where Pseudomonadales dominated about 95% of the gammaproteobacterial assemblage (Figure 3D). The Pseudomonadales order was also present in all other other samples, except for samples from sites 18 and 20, as well as sample 24F. Sample 24F also had an elevated dominance of Chromatiales (Gammaproteobacteria). Sample 04F also had a high abundance of the Methylococcales order (Figure 3D). Regarding Deltaproteobacteria, the Myxococcales order was abundant in most samples, except for a low abundance for samples 18M and 20M. For samples from site 20, a high dominance of Syntrophobacterales was recorded during both sampling events.

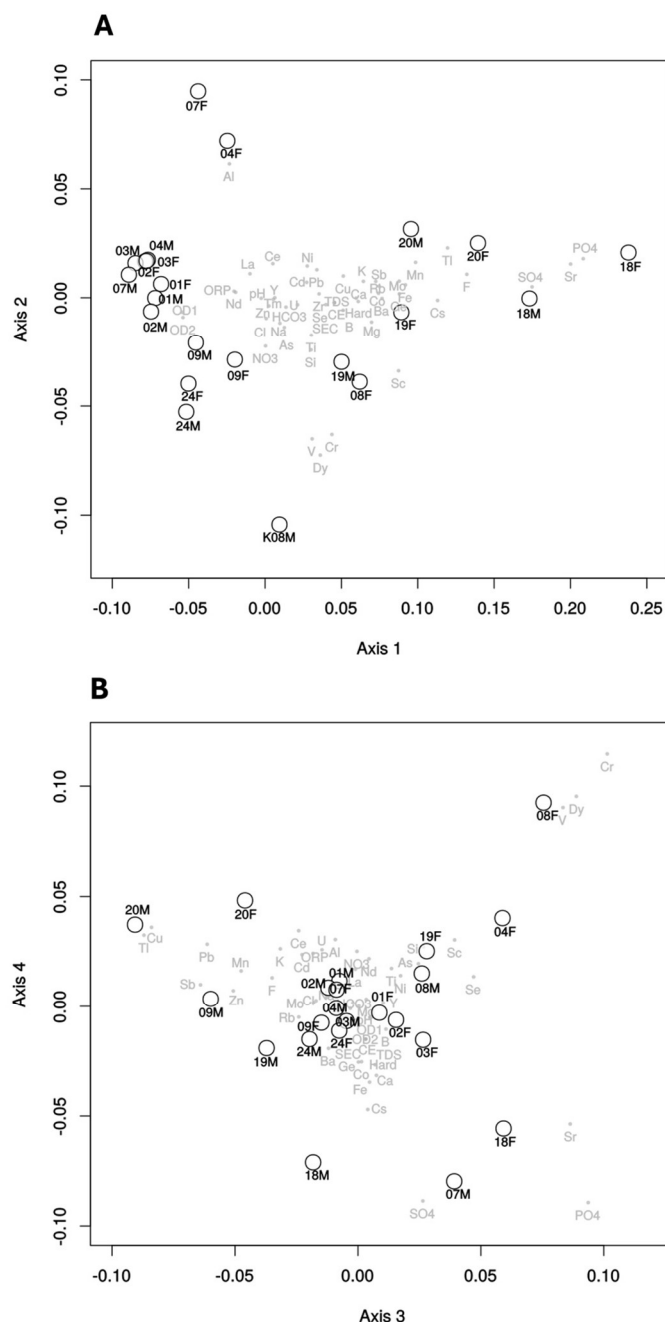


**Figure 2.** Principal coordinates ordination (PCO) of (A) the first and second axes and (B) the third and fourth axes of the environmental data set. Large black circles represent loadings for sample sites whereas small grey circles represent weighted averages for environmental variables. For codes of environmental variables, see Table 1.

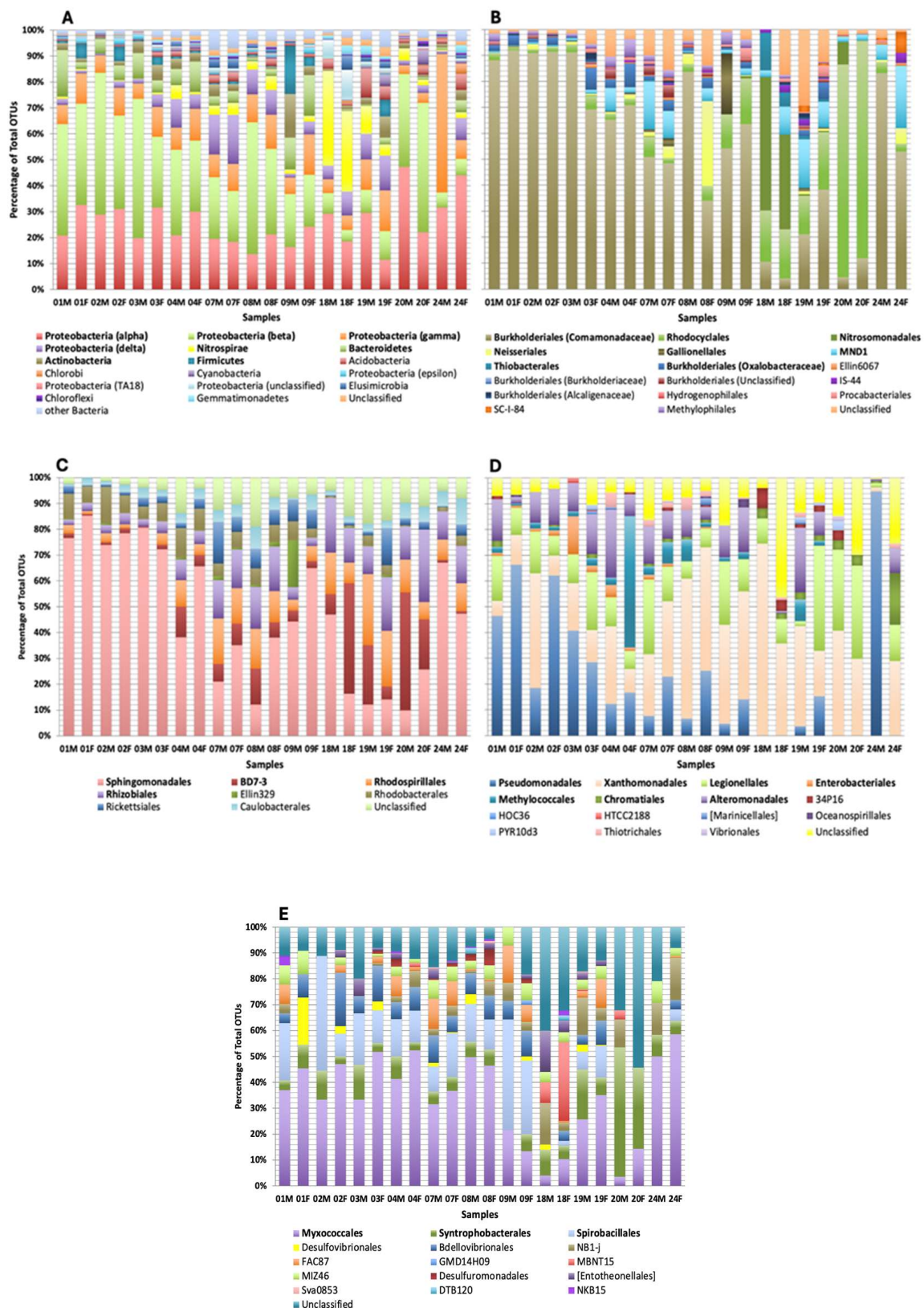


**Figure 3.** Relative abundance of bacterial 16S rDNA fragments from the Maciço Calcário Estremenho groundwater samples (with a contribution of 1% or more in at least one sample): (A) total bacteria at the phylum level, including Proteobacteria at the class level; (B) Betaproteobacteria at the order level; (C) Alphaproteobacteria at the order level; (D) Gammaproteobacteria at the order level; and (E) Deltaproteobacteria at the order level.



### 3.3. Analysis of Bacterial Community vs. Environmental Conditions

The first and third PCO axes of the environmental data set proved to be significant predictors of variation in composition, along with PCNM1, 2, 3, 4 and 7 (Table 2).

**Table 2.** Results of stepwise model building for constrained ordination for groundwater bacterial OTUs. Variable: explanatory variable, AIC: Aikake's Information Criterion, Perm: number of permutations.

Variable	Df	AIC	F	N. Perm	P
PCO3env	1	−9.7139	1.56	199	0.05
PCO1env	1	−7.2728	3.98	99	0.01
PCNM4	1	−7.5188	1.59	599	0.07
PCNM2	1	−7.5232	1.59	599	0.06
PCNM7	1	−7.3734	1.71	99	0.03
PCNM3	1	−7.2158	1.83	99	0.03
PCNM1	1	−6.7246	2.24	99	0.01

The dummy variable of the sampling event was not a significant predictor of variation in OTU composition; sites clustered together by location as opposed to the sampling event in the RDA analysis (Figure 4). The first and second axes shown in Figure 4 were both significant (axis 1:  $F_{1,14} = 5.42$ ,  $p = 0.005$ ; axis 2:  $F_{1,14} = 3.35$ ,  $p = 0.005$ ). OTU composition was primarily structured along a gradient related to PCO1 of the environmental analysis. Several OTUs were associated with sites with high RDA1 values and thus sites with high relative concentrations of Cs, Tl, F, Sr,  $SO_4$  and  $PO_4$  (Figures 2 and 4). These included OTUs 7, 8, 11, 14, 16, 20, 24, 27, 35 and 2109. OTU-7 assigned to the Rhodocyclales was closely related (sequence similarity > 99%) to an organism obtained from a well sediment sample. OTU-8 assigned to the order BD7-3 was closely related to an organism obtained from the effluent of a biodegrading process. OTU-11 assigned to the order Nitrospirales was related to an organism obtained from uranium mill tailings. The remaining OTUs assigned to taxa including the Rhizobiales, Nitrosomonadales and Xanthomonadales were related to organisms obtained from a cave groundwater, a drinking water system, a groundwater treatment filter, nitrification and denitrification reactors formed during the continuous supply of unchlorinated tap water, and sediment from slow sand filtration columns (Table 3).

OTUs with low RDA1 values and thus found in sites with high relative values of ORP, OD1 and OD2 included OTUs 2, 4, 9, 10, 15, 18, 19, 55 and 3070. These organisms assigned to taxa including the genera *Limnohabitans* and *Acidovorax* and the orders Sphingomonadales and Cytophagales were closely related (sequence similarity > 99%) to organisms obtained from river water, pumice, groundwater and lake water (Table 3). The second RDA axis was primarily related to PCNM1 and thus to large-scale spatial variation. Together, spatial and environmental variables explained 53% of the variation in composition, of which 30% was attributable to the purely spatial component, 17% due to the purely environmental component, and 6% due to the spatially structured environmental component.

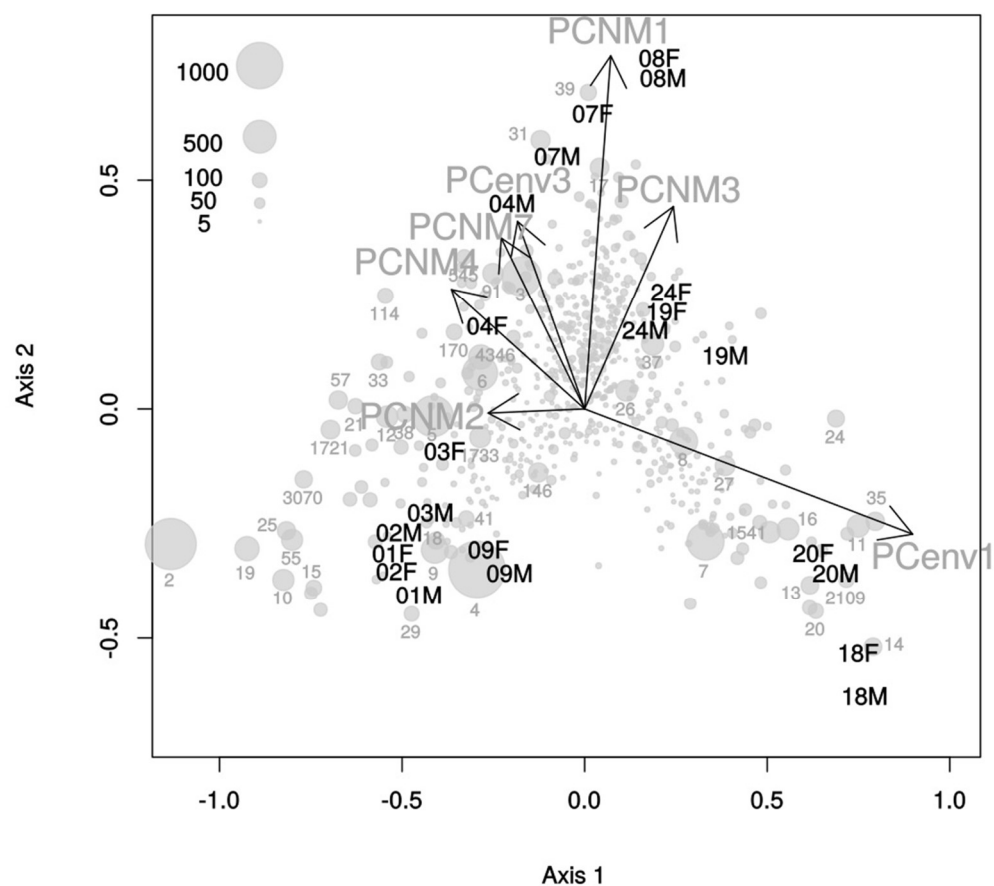


**Figure 4.** Ordination of OTU bacterial composition using redundancy analysis (RDA). OTU (small grey numbers), site (black codes) and environmental variables (large grey codes) are shown for the first and second axes. Arrows represent environmental variables, and their direction and length indicate their contribution to variation along those axes. For numbers relating to abundant ( $\geq 100$  sequences) OTUs, see Table 3.

**Table 3.** List of most abundant bacterial OTUs ( $\geq 100$  sequences) including OTU numbers; total sequences (Sum), taxonomic affiliation of OTU, GenBank GenInfo sequence identifiers (GI) of closely related organisms identified using BLAST; sequence identity (Sq ident) of these organisms with our representative OTU sequences; and isolation source (Source) of closely related organisms identified using BLAST.

OTU	Sum	Phylum	Class	Order	Family	Genus	GI	Sq. Ident (%)	Source
2	1215	Proteobacteria	Betaproteobacteria	Burkholderiales	Comamonadaceae	<i>Limnohabitans</i>	793958972	100	River water
3	717	Proteobacteria	Betaproteobacteria	Burkholderiales	Comamonadaceae	<i>Variovorax</i>	916346448	100	Rhizosphere soil, Greece: Katara Pass
4	1492	Proteobacteria	Alphaproteobacteria	Sphingomonadales	Unclassified	Unclassified	674124963	100	Pumice, Argentina: Lake Naheul Huapi
5	778	Proteobacteria	Alphaproteobacteria	Sphingomonadales	Sphingomonadaceae	<i>Novosphingobium</i>	511202206	99.75	Groundwater
6	568	Proteobacteria	Gammaproteobacteria	Pseudomonadales	Moraxellaceae	<i>Acinetobacter</i>	582054524	100	Holocene marine Sediment, China
7	640	Proteobacteria	Betaproteobacteria	Rhodocyclales	Rhodocyclaceae	<i>Sulfuritalea</i>	151547634	99.3	Well FW026 sediment sample, USA: Tennessee, Oak Ridge
8	358	Proteobacteria	Alphaproteobacteria	BD7-3	Unclassified	Unclassified	748047217	100	Thiocyanate and cyanate degrading bioprocess gold mining effluent
9	336	Proteobacteria	Betaproteobacteria	Burkholderiales	Comamonadaceae	<i>Acidovorax</i>	685431243	100	Groundwater from Qinghai-Tibet Plateau
10	205	Proteobacteria	Betaproteobacteria	Burkholderiales	Comamonadaceae	<i>Limnohabitans</i>	793958688	100	River water
11	231	Nitrospirae	Nitrospira	Nitrospirales	4-29	Unclassified	26005667	99.54	Uranium mill tailings, soil sample, USA: Shiprock, New Mexico
12	212	Bacteroidetes	Sphingobacteriia	Sphingobacteriales	Unclassified	Unclassified	583828438	100	Lake water, Japan: Yamanashi, Lake Mizugaki
13	142	Nitrospirae	Nitrospira	Nitrospirales	Unclassified	Unclassified	300383876	98.14	Saturated zone of the Hanford Site 300 Area subsurface, USA
14	143	Proteobacteria	Alphaproteobacteria	Rhizobiales	Hyphomicrobiaceae	<i>Parvibaculum</i>	411111333	99.26	FACE soil sample
15	112	Bacteroidetes	Cytophagia	Cytophagales	Cytophagaceae	Unclassified	793958725	100	River water
16	219	Proteobacteria	Unclassified	Unclassified	Unclassified	Unclassified	389621482	97.67	Water sample, USA: Carlsbad Caverns, New Mexico Room
17	160	Proteobacteria	Betaproteobacteria	Neisseriales	Neisseriaceae	<i>Vogesella</i>	648880879	100	Typha rhizosphere, China: Beijing, Chao Bai River
18	130	Bacteroidetes	Sphingobacteriia	Sphingobacteriales	Unclassified	Unclassified	184189928	99.29	Lake Michigan, USA: Wisconsin
19	272	Proteobacteria	Betaproteobacteria	Burkholderiales	Comamonadaceae	<i>Limnohabitans</i>	793958598	100	River water
20	102	Proteobacteria	Betaproteobacteria	Nitrosomonadales	Nitrosomonadaceae	Unclassified	190334133	99.77	Drinking water system, Greece: Trikala City
21	107	Proteobacteria	Betaproteobacteria	MND1	Unclassified	Unclassified	307098593	98.14	Aquifer, China: Mankyeong River
24	130	Proteobacteria	Gammaproteobacteria	Xanthomonadales	Sinobacteraceae	Unclassified	697252878	100	Sand filter material of groundwater treatment for drinking water supply, Denmark
25	149	Bacteroidetes	[Saprospirae]	[Saprospirales]	Chitinophagaceae	<i>Sediminibacterium</i>	310706589	99.53	Wetland
26	202	Proteobacteria	Alphaproteobacteria	Caulobacterales	Caulobacteraceae	Unclassified	696700883	100	Iodine (I-129) contaminated groundwater, USA: Hanford Site, Washington
27	180	Nitrospirae	Nitrospira	Nitrospirales	Nitrospiraceae	<i>Nitrospira</i>	761262239	100	Nitrification and denitrification reactors
29	101	Proteobacteria	Gammaproteobacteria	Xanthomonadales	Xanthomonadaceae	Unclassified	297179348	99.3	Lake Chaohu particle-attached bacteria sample
31	168	Proteobacteria	Betaproteobacteria	Unclassified	Unclassified	Unclassified	480542342	100	Sediment, Romania: Cave cu Apa din Valea Lesului
33	115	Proteobacteria	Betaproteobacteria	Burkholderiales	Comamonadaceae	<i>Rhodoferrax</i>	674125487	99.77	Pumice, Argentina: Lake Naheul Huapi
35	153	Proteobacteria	Alphaproteobacteria	BD7-3	Unclassified	Unclassified	387308169	100	Biofilm formed during continuous supply of unchlorinated tap water
37	227	Nitrospirae	Nitrospira	Nitrospirales	Nitrospiraceae	<i>Nitrospira</i>	519904151	100	Forest soil, Austria: Rothwald National Reserve
38	118	Actinobacteria	Acidimicrobiia	Acidimicrobiales	C111	Unclassified	674138767	100	Water, Argentina: Lake Naheul Huapi
39	121	Proteobacteria	Betaproteobacteria	Burkholderiales	Comamonadaceae	Unclassified	345466942	99.30	Rice paddy soil, Japan: Niigata
41	108	Firmicutes	Clostridia	Clostridiales	Clostridiaceae	<i>SMB53</i>	728803947	100	Cow manure
55	204	Proteobacteria	Betaproteobacteria	Burkholderiales	Comamonadaceae	<i>Limnohabitans</i>	471184987	100	Surface water of Lake Bosten, China
57	152	Proteobacteria	Betaproteobacteria	Burkholderiales	Comamonadaceae	<i>Rhodoferrax</i>	529085332	99.53	Villere Lake, France
91	187	Proteobacteria	Alphaproteobacteria	Sphingomonadales	Sphingomonadaceae	<i>Sphingomonas</i>	893670304	100	Mangrove rhizosphere, India
114	109	Proteobacteria	Betaproteobacteria	Burkholderiales	Comamonadaceae	<i>Hydrogenophaga</i>	674154381	100	Pumice, Argentina: Lake Naheul Huapi
146	169	Proteobacteria	Alphaproteobacteria	Sphingomonadales	Sphingomonadaceae	<i>Novosphingobium</i>	608789123	100	Sequencing batch reactor
170	114	Proteobacteria	Betaproteobacteria	Burkholderiales	Comamonadaceae	<i>Polaromonas</i>	422741017	100	Glacier, China
545	100	Proteobacteria	Alphaproteobacteria	Sphingomonadales	Sphingomonadaceae	<i>Kaistobacter</i>	556512094	100	Soil
1541	209	Proteobacteria	Betaproteobacteria	Rhodocyclales	Rhodocyclaceae	<i>Sulfuritalea</i>	472440156	99.77	Wetland
1721	161	Proteobacteria	Alphaproteobacteria	Sphingomonadales	Sphingomonadaceae	<i>Novosphingobium</i>	674199408	100	Water, Argentina: Lake Espejo
1733	201	Proteobacteria	Gammaproteobacteria	Pseudomonadales	Moraxellaceae	<i>Acinetobacter</i>	923095806	100	Soil
2109	103	Proteobacteria	Betaproteobacteria	Rhodocyclales	Rhodocyclaceae	<i>Sulfuritalea</i>	407313806	100	Sediment from slow sand filtration (SSF) columns,
3070	137	Proteobacteria	Alphaproteobacteria	Sphingomonadales	Unclassified	Unclassified	476000349	99.51	Mesotrophic artificial lake
4346	273	Proteobacteria	Gammaproteobacteria	Pseudomonadales	Moraxellaceae	<i>Acinetobacter</i>	630614109	100	<i>Acinetobacter johnsonii</i>

#### 4. Discussion

This study showed a high variation between samples in terms of both environmental parameters and bacterioplankton composition. Interestingly, samples from sampling sites 18 and 20 differed from other samples due to the absence of dissolved oxygen, indicating prevailing reducing conditions. Samples from site 18 also showed consistent groundwater quality across both seasons, including high electrical conductivity ( $1896\text{--}2001\text{ mS cm}^{-1}$ ) and TDS values (approximately  $1000\text{ mg L}^{-1}$ ). These values coincide with high Ca and  $\text{SO}_4$  concentrations, which may indicate that the origin of salinity is geogenic and related to the presence of gypsum in diapiric formations. Actually, these samples were collected at greater depths, specifically 297 and 233 m, for 18F (wet season) and 18M (dry season), respectively.

Anions such as Cl, F,  $\text{NO}_3$  and  $\text{NO}_2$  were within international drinking water standards [67], as well as cations Na, Mg and Fe, which had relatively low levels compared to those found in aquifers suffering mixing impact from saline intrusion [68] or from geogenic origin. As expected in karst formations,  $\text{HCO}_3$  levels ( $294\text{--}315\text{ mg L}^{-1}$ ) and Ca concentrations are high ( $445\text{--}500\text{ mg L}^{-1}$ ) due to calcite and other carbonate minerals dissolution. The extended drought periods that result in a scarcity of surface freshwaters and a shortage in the recharge and storage of groundwater, combined with an increased extraction pressure, can lead to an increase in total dissolved salts and groundwater quality issues, including geogenic salinisation. Although this is not the case, for coastal aquifers, salinisation can be further enhanced by saltwater intrusion [68], as already recorded in Southern Europe, from Italy (at Favignana Island [69]) to Portugal (at Central and Southern regions [25,70–72] and at the Islands of Graciosa and Pico [73]).

On the other hand, the lowest pH values (6.6) were recorded at samples from sites 18 and 20, in spite of not being below the drinking water guideline of 6.5 [68]. Nevertheless, these values suggest slightly acidic groundwaters that could affect the bacterial assemblages [74]. This may also indicate a trend for acidic pollution, usually linked to the oxidation of pyrite minerals, acid rain, and/or nitrification [75–77]. In fact, Fe concentrations in sample 18 ( $0.24\text{--}0.29\text{ mg L}^{-1}$ ) were close to the EPA standard drinking water limit of  $0.3\text{ mg L}^{-1}$ , but not at 20F ( $0.07\text{ mg L}^{-1}$ ). The high Fe levels can be explained by the fact that Fe is highly soluble in acidic environments and can also be cycled by acidophile microorganisms. Other high soluble metals and metalloids were also either undetectable or showed relatively low levels, such as Al or Mn, below the EPA limits of  $20\text{ mg L}^{-1}$  and  $50\text{ mg L}^{-1}$  [68], in these samples. The same was true for  $\text{NO}_3$  and  $\text{NO}_2$  concentrations, which were below  $0.50\text{ mgN L}^{-1}$  and undetectable, respectively, at site 18, although  $\text{NO}_3$  could reach  $3.73\text{ mgN L}^{-1}$  at 20F. Increased nitrate levels have been associated with groundwater pollution [78,79] through the leaching of effluents from animal manure and slurry application in soils. Another particular result was the high concentration of Sr ( $9.70\text{ mg L}^{-1}$ ) recorded in sample 18F, way above the guideline value of  $1.5\text{ mg L}^{-1}$  [68], also suggesting geogenic origin. Interestingly, in February, sample 19F also yielded a high value of Sr ( $2.30\text{ mg L}^{-1}$ ), suggesting a possible connection between sampling sites 18 and 19 during the wet season, when these high levels occurred. Moreover, instead of a potential washing of some solutes during the wet season, resulting in lower concentrations and accumulation during the dry season, samples showed pronounced concentrations of most solutes during the wet season and lower concentrations in the drier period. This suggests a deeper circulation and mixing of contamination during the rainy season. Actually, Valverde–Alcanede is a region of intense mining and extractive industrial activity, which contributes extensively to contamination with metals. Moreover, karst areas are formed by an underground drainage system formed by fissures and conduits that make these environments prone to contamination from point and diffuse sources of surface pollution, with a major impact on groundwater ecosystems [80,81].

Bacteria are a key community in every aquatic ecosystem, with an important role in environmental processes, namely energy and nutrient cycling, and bacterial community composition can vary under diverse environmental conditions, thus acting as bioindicator of water quality [82,83], especially after strong changes in the aquatic ecosystems. In fact,



the present study shows a high bacterial diversity across samples (as previously reported for other Portuguese groundwater samples [33,35]) but also an important variation of bacterial community composition according to the hydrogeochemistry (among sites and/or between the two seasons). At some sites (e.g., 9, 18, 19, 20 and 24), the seasonal variability was significant, which suggested a higher vulnerability of these aquifer spots to impacts, either from geohydrological conditions or from potential surface contamination. In fact, Tiago and Veríssimo [35] and França et al. [33] also reported variations in Portuguese groundwater bacterial assemblages between samples collected in wet and dry seasons.

The dominance of Proteobacteria was massive across the studied Estremenho groundwater samples (ranging between 43.3–92.1% of total OTUs), which is frequently reported in freshwater bodies across the globe, including diverse Portuguese surface freshwaters [48,50,84,85] but also groundwaters [33,35]. For Betaproteobacteria, the order Burkholderiales was dominant in most samples, particularly members assigned to the family Comamonadaceae and genus *Limnohabitans* (with different OTUs affiliating with sequences from riverine waters), followed by other genera such as *Acidovorax* (from groundwater), *Rhodoferax* and *Hydrogenophaga* (from freshwater lakes), *Variovorax* (from rhizosphere soil) or even *Polaromonas* (from a glacier). In fact, the dominance of Comamonadaceae bacteria has been reported as ubiquitous under diverse conditions [86], including contaminated groundwaters rich in sulfide or As [32,82]. The genus *Rhodoferax* has been associated with the transformation of Fe and  $\text{SO}_4$  [87]. *Limnohabitans*, *Variovorax*, *Hydrogenophaga* and *Acidovorax* strains, in particular, have been found in high nitrate and/or ammonia groundwaters [88–90]. *Polaromonas* strains are also involved in the nitrogen and carbon cycles [91]. However, for sites 18 and 20, respectively, Nitrosomonadales and Rhodocyclales were the most abundant betaproteobacterial orders. Then again, for both these sites, the hydrogeochemical features that suggested groundwater contamination, under anaerobic conditions, also had an impact on the bacterial assemblages recorded. For sampling site 18, the dominant Nitrosomonadales OTU was assigned to a strain of Nitrosomonadaceae from drinking water. Interestingly, sampling site 18 also had a dominance of the class Nitrospirales. Members of Nitrosomonadales (e.g., *Nitrosomonas* strains) as well as Nitrospirales (e.g., *Nitrospira* strains) are associated with nitrification and are included in an ammonia-oxidizing bacteria (AOB) group found in aerobic environments and have been recorded at both low and high depths [92,93], playing a major role in the cycle of nitrogen, by oxidizing ammonia to nitrite and, ultimately, allowing the conversion of nitrite into nitrate [94,95]. Nitrosomonadales bacteria have been linked to ammonia oxidation, whereas Nitrospirales members have been associated with the transformation of nitrite to nitrate [30] and are often referred also as nitrite-oxidizing bacteria (NOB) [94]. However, under anaerobic conditions, the oxidation of ammonia (anammox) leads to the formation of dinitrogen gas ( $\text{N}_2$ ) [96,97]. In fact, this could be the case at samples from site 18, as oxygen levels and nitrite concentrations were undetectable, and nitrate was only detectable at a low concentration at 18F ( $0.48 \text{ mgN L}^{-1}$ ). On the other hand, *Nitrosomonas* strains can be found from marine water to anaerobic sediments and are also dominant in sand filters from drinking water treatment plants [95,98], including biofilters for removing Fe and Mn from groundwaters [99,100], as well as in As-rich groundwaters also with high ammonium, Fe and/or Mn concentrations [93,101,102], thus also indicating their ability to persist and multiply in groundwaters suffering inorganic pollution. *Nitrospira* has been also detected in Portuguese aquifers with either oligotrophic features [33] or high alkalinity with undetectable oxygen levels [35]. Interestingly, samples from site 18 showed anaerobic conditions and concentrations of Mn ( $2.1\text{--}2.6 \text{ mg L}^{-1}$ ) surpassing the drinking water guideline of  $0.1 \text{ mg L}^{-1}$  and also increased Fe concentrations ( $0.24\text{--}0.29 \text{ mg L}^{-1}$ ) near the drinking water guideline of  $0.30 \text{ mg L}^{-1}$ , although As levels were not very high ( $\leq 0.25 \text{ mg L}^{-1}$ ). Nevertheless, results suggest a trend for inorganic pollution at site 18, which can also be a major concern for drinking water supply [100–102].  $\text{PO}_4$  levels were also very high for sample 18F ( $0.93 \text{ mg L}^{-1}$ ), exceeding the recommended value of  $0.025 \text{ mg L}^{-1}$  [68]. High concentrations of  $\text{NO}_3$  and  $\text{PO}_4$  are usually related to anthropogenic activities such as intensive agriculture and animal farm-

ing [78,79]. At samples 18, the presence of Gammaproteobacteria Xanthomonadales and the candidate lineage MBNT 15 was also very representative. Whereas Xanthomonadales bacteria have been linked to ammonia-oxidation environments [94], MBNT 15 bacteria have been referred to as anaerobic sulfate-reducing bacteria (SRB) [103]. This is in concordance with the highest  $\text{SO}_4$  levels attained at these groundwater samples (933–1100  $\text{mg L}^{-1}$ ), largely surpassing the international safety guideline of 250  $\text{mg L}^{-1}$ , along with the lack of oxygen in samples, as previously mentioned.

On the other hand, for samples 20F and 20M, there was a massive dominance of betaproteobacteria Rhodocyclales assigned to the genus *Sulfuritalea*. Strains of this genus have been related to the oxidation of sulfur compounds and denitrification (of nitrate to  $\text{N}_2\text{O}$  or  $\text{N}_2$  gas), in both pristine [104–106] and contaminated aquifers that are rich in nitrate, As, Mn and/or Fe [107–110]. In fact, at site 20, nitrate levels were higher than in most samples, ranging from 3.65 to 3.75  $\text{mg L}^{-1}$ , although still below the drinking water guideline of 10  $\text{mg L}^{-1}$ . However, denitrification usually occurs in aerobic conditions, but it can also occur in anaerobiosis [106,108,111,112], which seems to be the case under the absence of oxygen recorded in these samples. Here, despite the low Fe levels (0.07–0.09  $\text{mg L}^{-1}$ ), Mn reached 7.1  $\text{mg L}^{-1}$  in sample 20F, surpassing the drinking water guideline of 0.1  $\text{mg L}^{-1}$ .

For both sites 18 and 20, OTUs matching Alphaproteobacteria members from BD7–3 (from a biofilm formed in a tap water supply), Sphingomonadales (*Novosphingobium* genus from freshwaters), Rhizobiales (genus *Parvibaculum* from soil) and Rhodospirillales orders were also dominant. Rhizobiales members (e.g., *Nitrobacter*) have also been linked to nitrite oxidation [32], whereas Sphingomonadales members include ammonia-oxidizing bacteria, which are dominant in contaminated groundwaters [113] and under anaerobic conditions [92], as recorded for these samples. Rhodospirillales members have been related to aquifers also with low oxygen and contamination from dairy farming [114]. BD7–3 and *Novosphingobium* bacteria have been previously reported dominating together in As-contaminated groundwaters [115].

The dominance of the Methylococcales order within the Gammaproteobacteria was recorded at sample 04F, with dominant taxa belonging to the genera *Methylomonas* and *Crenothrix*. *Methylomonas* strains are methylotrophic but have been also related to denitrification, along with *Sulfuritalea* bacteria [108]. This order has also been associated with As-rich groundwaters [116], namely the *Crenothrix* genus [117]. However, there were no particular hydrogeochemical parameters that could be directly associated with this dominance.

Multivariate analyses also evidenced a clear separation of samples from sites 08 and 07. In fact, samples from site 08 were shown to be rich in several elements, including peaks of Si (15.2–15.5  $\text{mg L}^{-1}$ ), Sc (4  $\text{mg L}^{-1}$ ), Ti (2.4–2.5  $\text{mg L}^{-1}$ ), V (15.9–16.9  $\text{mg L}^{-1}$ ) and Cr (1.0–1.8  $\text{mg L}^{-1}$ ), but they also showed relevant nitrate levels (6.34–8.37  $\text{mg L}^{-1}$ ), although within the guideline of 11.3  $\text{mgN L}^{-1}$ , highlighting once more the potential contamination from urban drainage, sewers and agricultural activities at the Maciço Calcário Estremenho [34,47,78,79]. However, the Neisseriales order (Betaproteobacteria) was very representative only at 08F, when the dissolved oxygen levels were lower (2.8  $\text{mg L}^{-1}$ ) and Sr concentration was higher (0.40  $\text{mg L}^{-1}$ ). Sample 07F showed the highest Al levels (59  $\text{mg L}^{-1}$ ), above the guideline of 20  $\text{mg L}^{-1}$ , but neither 07 sample showed drastic changes in their bacterial composition, characterized by a diverse and dominance-shared bacterial composition.

A particular bacterioplankton composition was recorded at sample 24M, with the almost total dominance of the Pseudomonadales (Gammaproteobacteria), matching an *Acinetobacter johnsonii* sequence. Gammaproteobacteria have been frequently associated with contaminated groundwaters [34,82]. *Acinetobacter* strains, in particular, have been reported as dominant in groundwater samples with both low and high As levels [113,118], and have been also associated with the dissolution of magnetite and higher levels of Fe, indirectly promoting the reduction of nitrate by autotrophic denitrifying bacteria [119]. However, although sample 24M presented relatively high  $\text{NO}_3$  levels (4.77  $\text{mg L}^{-1}$ ), suggesting contamination from the surface [34], the concentrations of As and Fe were undetectable and

below  $0.05 \text{ mg L}^{-1}$ , respectively. Gammaproteobacteria OTUs assigned to orders Legionellales and Alteromonadales were also well represented in most samples. The Legionellales order includes *Legionella*, a genus that has been linked to serious health risks and that has also been found in aquifers across Europe, including in Portugal [40,120]. Alteromonadales members have been associated with marine environments or groundwaters suffering salinization [121], with high levels of Cl, Na, Mg and  $\text{SO}_4$ . Deltaproteobacteria from the order Myxococcales were also dominant across most samples, except for samples 18 and 20, suggesting their preference for aerobic environments, as previously reported [122].

Other dominant OTUs across the groundwater samples were assigned to phyla Bacteroidetes (Cytophagales and Saprospirales orders), Actinobacteria (Acidimicrobiales order) and Firmicutes (Clostridiales order), which are frequent in groundwaters [116]. Bacteroidetes dominance has previously been related to increased concentrations of  $\text{SO}_4$ , TDS and Si [123]. Actinobacteria are ubiquitous across freshwaters, but Acidimicrobiales (family C111) members have been also detected in groundwaters [124]. Firmicutes was dominated by an OTU affiliated with a sequence from the Clostridiales order and genus SMB53 retrieved from cow manure. In fact, SMB53 has been previously associated with groundwater contaminated from leachates related to livestock activities, showing high EC, Cl and  $\text{SO}_4$  [125].

## 5. Conclusions

This study brings new information on the bacterial community composition from Portuguese groundwaters, particularly from the Maciço Calcário Estremenho aquifer, located in Central Western Portugal. The variation in the bacterioplankton community suggests seasonal responses to diverse hydrogeochemical conditions, with a general trend indicating contamination from the surface. During the dry season, there was a general decrease in peak concentrations recorded in February for some elements (e.g., Ni, Al, Ba, As, F, Sr, Mn), showing the influence of precipitation through the drainage of surface contaminants into the aquifer. The contamination from surface leachates derived from urban drainage and agricultural activities has been previously reported at the Maciço Calcário Estremenho Karst Massif. Dissolved oxygen and ORP, as well as concentrations of Sr,  $\text{SO}_4$ ,  $\text{PO}_4$ , Al, V, Cr, Fe, Cl, Cu, Pb, Mn and Zn, were the main parameters that could explain most of the bacterial structure variability among samples. Dominant recorded OTUs were generally related to bacteria found in contaminated groundwaters, usually rich in As, Fe, Mn,  $\text{SO}_4$  and/or nitrate, including genera *Limnohabitans*, *Acidovorax*, *Variovorax*, *Hydrogenophaga*, *Rhodoferrax*, *Polaromonas*, *Sulfuritalea*, *Novosphingobium*, *Parvibaculum*, *Methylobacter*, *Crenothrix* and *Acinetobacter*, but also members of the orders Xanthomonadales, Neisseriales, Legionellales, Alteromonadales, Cytophagales, Saprospirales, Acidimicrobiales and Clostridiales, as well as the candidate lineage MBNT 15 and BD7-3, suggesting the potential importance of these bacterial assemblages on the migration and transformation of these contaminants. In fact, the bacterial assemblages gathering diverse bacteria with major roles in the different biogeochemical cycles can act synergistically to significantly decrease the concentrations of contaminants such as nitrate, arsenic or sulfide, as reported previously [112].

Our findings are an important baseline for future studies or monitoring programs for Southern Europe, which is under the increasing pressure of severe climate change episodes that impact groundwater ecosystems. The present work also gives exploratory insights into the use of bacteria as a key community to track environmental variations in groundwater quality. DNA metabarcoding approaches may thus provide critical information for bacterial diversity in these still unknown ecosystems. Moreover, instead of using solely analyses of pathogenic and toxic bacteria, the integration of information on the whole bacterial community should be seriously considered in the future as part of integrated routine water quality assessment and monitoring programs, as previously suggested [82].

**Author Contributions:** Conceptualization, D.R.d.F.; methodology, D.R.d.F., D.F.R.C. and M.T.C.d.M.; software analysis, D.F.R.C. and A.R.M.P.; validation, M.T.C.d.M., N.A. and D.R.d.F.; investigation, D.R.d.F., M.T.C.d.M., A.R.M.P., P.P.S., J.O. and A.M.M.G.; funding acquisition, N.A. and A.S.P.S.R.;

data curation, M.T.C.d.M., D.R.d.F. and D.F.R.C.; writing—original draft preparation, D.R.d.F.; writing—review and editing, D.R.d.F., M.T.C.d.M., A.R.M.P., P.P.S., D.F.R.C., N.A., A.M.M.G. and A.S.P.S.R.; visualization, D.R.d.F. and D.F.R.C. All authors have read and agreed to the published version of the manuscript.

**Funding:** This work had financial support from the Portuguese Foundation for Science and Technology (FCT) which funded the project KARSTRISK (PTDC/AAC-AMB/114781/2009), a post-doc grant SFRH/BPD/74184/2010 and a research contract for D.R.F. supported by FCT/national funds (OE), according to the DL 57/2016 (<https://doi.org/10.54499/DL57/2016/CP1482/CT0034>). A.R.M.P. was also supported by a postdoctoral scholarship (SFRH/BPD/117563/2016) funded by FCT/national funds (MCTES) and by the European Social Fund (ESF)/EU. Other funding came from national funds FCT/MCTES and FEDER (PT2020 Partnership Agreement and Compete 2020) to CESAM UIDP/50017/2020+UIDB/50017/2020+ LA/P/0094/2020) and cE3c (UIDB/00329/2020). A.M.M.G. also acknowledges the University of Coimbra for the contract IT057–18-7253 and the Centre for Functional Ecology-Science for People and the Planet (CFE/UIDB/04004/2020; <https://doi.org/10.54499/UIDB/04004/2020>), financed by FCT/MCTES through national funds (PIDDAC) and Associate Laboratory TERRA (LA/P/0092/2020; <https://doi.org/10.54499/LA/P/0092/2020>).

**Data Availability Statement:** Raw sequence data were submitted to NCBI under BioProject ID PRJNA1009823.

**Conflicts of Interest:** The authors declare no conflicts of interest.

## References

- Deng, J.; Qin, B.; Paerl, H.W.; Zhang, Y.; Ma, J.; Chen, Y. Earlier and Warmer Springs Increase Cyanobacterial (*Microcystis* spp.) Blooms in Subtropical Lake Taihu, China. *Freshw. Biol.* **2014**, *59*, 1076–1085. [[CrossRef](#)]
- Qin, B.; Deng, J.; Shi, K.; Wang, J.; Brookes, J.; Zhou, J.; Zhang, Y.; Zhu, G.; Paerl, H.W.; Wu, L. Extreme Climate Anomalies Enhancing Cyanobacterial Blooms in Eutrophic Lake Taihu, China. *Water Resour. Res.* **2021**, *57*, e2020WR029371. [[CrossRef](#)]
- de Figueiredo, D.R. Harmful Cyanobacterial Blooms: Going beyond the “Green” to Monitor and Predict HCBs. *Hydrobiology* **2024**, *3*, 11–30. [[CrossRef](#)]
- Priya, A.K.; Muruganandam, M.; Rajamanickam, S.; Sujatha, S.; Madhava, K.R.G.; Priya, V.; Gomathi, R.; Gokulan, R.; Thirumala, R.G.; Senthil, K.M. Impact of Climate Change and Anthropogenic Activities on Aquatic Ecosystem—A Review. *Environ. Res.* **2023**, *238*, 117233.
- de Vicente, I. Biogeochemistry of Mediterranean Wetlands: A Review about the Effects of Water-Level Fluctuations on Phosphorus Cycling and Greenhouse Gas Emissions. *Water* **2021**, *13*, 1510. [[CrossRef](#)]
- Ondrasek, G.; Rengel, Z. Environmental Salinization Processes: Detection, Implications & Solutions. *Sci. Total Environ.* **2021**, *754*, 142432. [[PubMed](#)]
- Pinkney, A.E.; Driscoll, C.T.; Evers, D.C.; Hooper, M.J.; Horan, J.; Jones, J.W.; Lazarus, R.S.; Marshall, H.G.; Milliken, A.; Rattner, B.A.; et al. Interactive Effects of Climate Change with Nutrients, Mercury, and Freshwater Acidification on Key Taxa in the North Atlantic Landscape Conservation Cooperative Region. *Integr. Environ. Assess. Manag.* **2015**, *11*, 355–369. [[CrossRef](#)] [[PubMed](#)]
- Mosley, L.M. Drought Impacts on the Water Quality of Freshwater Systems; Review and Integration. *Earth Sci. Rev.* **2015**, *140*, 203–214. [[CrossRef](#)]
- Chen, X.; Sheng, Y.; Wang, G.; Zhou, P.; Liao, F.; Mao, H.; Zhang, H.; Qiao, Z.; Wei, Y. Spatiotemporal Successions of N, S, C, Fe, and As Cycling Genes in Groundwater of a Wetland Ecosystem: Enhanced Heterogeneity in Wet Season. *Water Res.* **2024**, *251*, 121105. [[CrossRef](#)]
- Pronk, M.; Goldscheider, N.; Zopfi, J. Particle-Size Distribution As Indicator for Fecal Bacteria Contamination of Drinking Water from Karst Springs. *Environ. Sci. Technol.* **2007**, *41*, 8400–8405. [[CrossRef](#)]
- Schmidt, S.; Geyer, T.; Marei, A.; Guttman, J.; Sauter, M. Quantification of Long-Term Wastewater Impacts on Karst Groundwater Resources in a Semi-Arid Environment by Chloride Mass Balance Methods. *J. Hydrol.* **2013**, *502*, 177–190. [[CrossRef](#)]
- Hynds, P.; Misstear, B.D.; Gill, L.W.; Murphy, H.M. Groundwater Source Contamination Mechanisms: Physicochemical Profile Clustering, Risk Factor Analysis and Multivariate Modelling. *J. Contam. Hydrol.* **2014**, *159C*, 47–56. [[CrossRef](#)]
- Saccò, M.; Mammola, S.; Altermatt, F.; Alther, R.; Bolpagni, R.; Brancelj, A.; Brankovits, D.; Fišer, C.; Gerovasileiou, V.; Griebler, C.; et al. Groundwater is a hidden global keystone ecosystem. *Glob. Chang. Biol.* **2024**, *30*, e17066. [[CrossRef](#)]
- Grimmeisen, F.; Zemmann, M.; Goeppert, N.; Goldscheider, N. Weekly Variations of Discharge and Groundwater Quality Caused by Intermittent Water Supply in an Urbanized Karst Catchment. *J. Hydrol.* **2016**, *537*, 157–170. [[CrossRef](#)]
- Worthington, S.R.H.; Smart, C.C. Transient Bacterial Contamination of the Dual-Porosity Aquifer at Walkerton, Ontario, Canada. *Hydrogeol. J.* **2017**, *25*, 1003–1016. [[CrossRef](#)]
- Knierim, K.J.; Hays, P.D.; Bowman, D. Quantifying the Variability in Escherichia Coli (E. Coli) throughout Storm Events at a Karst Spring in Northwestern Arkansas, United States. *Environ. Earth Sci.* **2015**, *74*, 4607–4623. [[CrossRef](#)]



17. Fakhreddine, S.; Prommer, H.; Scanlon, B.R.; Ying, S.C.; Nicot, J.P. Mobilization of Arsenic and Other Naturally Occurring Contaminants during Managed Aquifer Recharge: A Critical Review. *Environ. Sci. Technol.* **2021**, *55*, 2208–2223. [[CrossRef](#)]
18. Reiss, J.; Perkins, D.M.; Fussmann, K.E.; Krause, S.; Canhoto, C.; Romeijn, P.; Robertson, A.L. Groundwater Flooding: Ecosystem Structure Following an Extreme Recharge Event. *Sci. Total Environ.* **2019**, *652*, 1252–1260. [[CrossRef](#)]
19. Mammola, S.; Cardoso, P.; Culver, D.C.; Deharveng, L.; Ferreira, R.L.; Fišer, C.; Galassi, D.P.M.; Griebler, C.; Halse, S.; Humphreys, W.F.; et al. Scientists' warning on the conservation of subterranean ecosystems. *BioScience* **2019**, *69*, 641–650. [[CrossRef](#)]
20. Drew, D.P.; Hötzl, H. *Karst Hydrogeology and Human Activities: Impacts, Consequences and Implications*; A.A. Balkema: Rotterdam, The Netherlands, 1999; ISBN 9054104635/9789054104636.
21. Gutiérrez, F.; Parise, M.; De Waele, J.; Jourde, H. A Review on Natural and Human-Induced Geohazards and Impacts in Karst. *Earth Sci. Rev.* **2014**, *138*, 61–88. [[CrossRef](#)]
22. Bartolini, G.; Grifoni, D.; Magno, R.; Torrigiani, T.; Gozzini, B. Changes in Temporal Distribution of Precipitation in a Mediterranean Area (Tuscany, Italy) 1955–2013. *Int. J. Climatol.* **2018**, *38*, 1366–1374. [[CrossRef](#)]
23. Danielopol, D.A.N.L.; Griebler, C.; Gunatilaka, A.; Notenboom, J. Present State and Future Prospects for Groundwater Ecosystems. *Environ. Conserv.* **2003**, *30*, 104–130. [[CrossRef](#)]
24. Ford, D.; Williams, P.D. *Karst Hydrogeology and Geomorphology*, Hall, C., Ed.; Wiley: Hoboken, NJ, USA, 2007; ISBN 9780470060056.
25. do Nascimento, T.V.M.; de Oliveira, R.P.; Condesso de Melo, M.T. Impacts of Large-Scale Irrigation and Climate Change on Groundwater Quality and the Hydrological Cycle: A Case Study of the Alqueva Irrigation Scheme and the Gabros de Beja Aquifer System. *Sci. Total Environ.* **2024**, *907*, 168151. [[CrossRef](#)] [[PubMed](#)]
26. Costa, L.R.D.; Hugman, R.T.; Stigter, T.Y.; Monteiro, J.P. Predicting the Impact of Management and Climate scenarios on Groundwater Nitrate Concentration Trends in Southern Portugal. *Hydrogeol. J.* **2021**, *29*, 2501–2616. [[CrossRef](#)]
27. Haack, T.K.; McFeters, G.A. Microbial Dynamics of an Epilithic Mat Community in a High Alpine Stream. *Appl. Environ. Microbiol.* **1982**, *43*, 702–707. [[CrossRef](#)]
28. Alfreider, A.; Psenner, R.; Amann, R. Seasonal Community and Population Dynamics of Pelagic Bacteria and Archaea in a High Mountain Lake. *Society* **1998**, *64*, 4299–4306.
29. Farnleitner, A.H.; Wilhartitz, I.; Ryzinska, G.; Kirschner, A.K.T.; Stadler, H.; Burtscher, M.M.; Hornek, R.; Szewzyk, U.; Herndl, G.; Mach, R.L. Bacterial Dynamics in Spring Water of Alpine Karst Aquifers Indicates the Presence of Stable Autochthonous Microbial Endokarst Communities. *Environ. Microbiol.* **2005**, *7*, 1248–1259. [[CrossRef](#)]
30. Borsodi, A.K.; Anda, D.; Szabó, A.; Megyes, M.; Krett, G. Impacts of Different Habitats on the Composition of Bacterial Communities at the Discharging Endpoints of a Hypogene Thermal Karst System. *Geomicrobiol. J.* **2022**, *39*, 155–165. [[CrossRef](#)]
31. Adesso, R.; Gonzalez-Pimentel, J.L.; D'angeli, I.M.; De Waele, J.; Saiz-Jimenez, C.; Jurado, V.; Miller, A.Z.; Cubero, B.; Vigliotta, G.; Baldantoni, D. Microbial Community Characterizing Vermiculinations from Karst Caves and Its Role in Their Formation. *Microb. Ecol.* **2021**, *81*, 884–896. [[CrossRef](#)]
32. Anda, D.; Szabó, A.; Kovács-Bodor, P.; Makk, J.; Felföldi, T.; Ács, É.; Mádl-Szőnyi, J.; Borsodi, A.K. In Situ Modelling of Biofilm Formation in a Hydrothermal Spring Cave. *Sci. Rep.* **2020**, *10*, 884–896. [[CrossRef](#)]
33. França, L.; Lopéz-Lopéz, A.; Rosselló-Móra, R.; da Costa, M.S. Microbial Diversity and Dynamics of a Groundwater and a Still Bottled Natural Mineral Water. *Environ. Microbiol.* **2015**, *17*, 577–593. [[CrossRef](#)]
34. Garcia-Sanchez, A.M.; Miller, A.Z.; Jurado, V.; Dionisio, D.; Muralha, V.S.F.; Afonso, M.J.; Chamine, H.I. Is the Presence of Bacterial Communities Related to the Urban Contamination Sources of the 16th Century Paranhos Spring Water Tunnel? In *The Conservation of Subterranean Cultural Heritage*; CRC Press: Boca Raton, FL, USA, 2014; pp. 95–102.
35. Tiago, I.; Veríssimo, A. Microbial and Functional Diversity of a Subterrestrial High pH Groundwater Associated to Serpentinization. *Environ. Microbiol.* **2013**, *15*, 1687–1706. [[CrossRef](#)] [[PubMed](#)]
36. Teixeira, P.; Dias, D.; Costa, S.; Brown, B.; Silva, S.; Valério, E. *Bacteroides* spp. and Traditional Fecal Indicator Bacteria in Water Quality Assessment—An Integrated Approach for Hydric Resources Management in Urban Centers. *J. Environ. Manag.* **2020**, *271*, 110989. [[CrossRef](#)]
37. Teixeira, P.; Almeida, L.; Brandão, J.; Costa, S.; Pereira, S.; Valério, E. Non-Potable Use of Lisbon Underground Water: Microbiological and Hydrochemical Data from a 4-Year Case Study. *Environ. Monit. Assess.* **2018**, *190*, 455. [[CrossRef](#)] [[PubMed](#)]
38. Araújo, S.; Silva, I.A.; Tação, M.; Patinha, C.; Alves, A.; Henriques, I. Characterization of Antibiotic Resistant and Pathogenic *Escherichia coli* in Irrigation Water and Vegetables in Household Farms. *Int. J. Food Microbiol.* **2017**, *257*, 192–200. [[CrossRef](#)] [[PubMed](#)]
39. Cruz, J.V.; Pacheco, D.; Cymbron, R.; Mendes, S. Monitoring of the Groundwater Chemical Status in the Azores Archipelago (Portugal) in the Context of the EU Water Framework Directive. *Environ. Earth Sci.* **2010**, *61*, 173–186. [[CrossRef](#)]
40. Costa, J.; Tiago, I.; Da Costa, M.S.; Veríssimo, A. Presence and Persistence of *Legionella* spp. in Groundwater. *Appl. Environ. Microbiol.* **2005**, *71*, 663–671. [[CrossRef](#)]
41. Tiago, I.; Chung, A.P.; Veríssimo, A. Bacterial Diversity in a Nonsaline Alkaline Environment: Heterotrophic Aerobic Populations. *Appl. Environ. Microbiol.* **2004**, *70*, 7378–7387. [[CrossRef](#)]
42. Hugenholtz, P. Exploring Prokaryotic Diversity in the Genomic Era. *Genome Biol.* **2002**, *3*, reviews0003.1–reviews0003.8. [[CrossRef](#)]
43. Rodrigues, M.L. The Limestone Massif of Estremadura. In *Landscapes and Landforms of Portugal. World Geomorphological Landscapes*; Vieira, G., Zêzere, J., Mora, C., Eds.; Springer: Cham, Switzerland, 2020. [[CrossRef](#)]

44. Bilha, J.; Andrade, C.; Azerêdo, A.; Barriga, F. Definition of the Portuguese Frameworks with International Relevance as an Input for the European Geological Heritage Characterisation. *Episodes* **2005**, *28*, 177–186. [[CrossRef](#)] [[PubMed](#)]
45. Azerêdo, A.C. Formal Lithostratigraphy of the Lower and Middle Jurassic from the Maciço Calcário Estremenho (Lusitanian Basin) [Formalização Da Litostratigrafia Do Jurássico Inferior e Médio Do Maciço Calcário Estremenho (Bacia Lusitânica)]. *Comun. Geológicas* **2007**, *94*, 29–51.
46. Machado, S.; Mergulhão, L.; Pereira, B.C.; Pereira, P.; Carvalho, J.; Anacleto, J.A.; de Carvalho, C.N.; Belo, J.; Paredes, R.; Baucon, A. Geoconservation in the Cabeço Da Ladeira Paleontological Site (Serras de Aire e Candeeiros Nature Park, Portugal): Exquisite Preservation of Animals and Their Behavioral Activities in a Middle Jurassic Carbonate Tidal Flat. *Geosciences* **2021**, *11*, 366. [[CrossRef](#)]
47. Reboleira, A.S.P.S.; Borges, P.; Gonçalves, F.; Serrano, A.; Oromí, P. The subterranean fauna of a biodiversity hotspot region—Portugal: An overview and its conservation. *Int. J. Speleol.* **2011**, *40*, 23–37. [[CrossRef](#)]
48. de Figueiredo, D.R.; Pereira, M.J.; Correia, A. Seasonal Modulation of Bacterioplankton Community at a Temperate Eutrophic Shallow Lake. *World J. Microbiol. Biotechnol.* **2010**, *26*, 1067–1077. [[CrossRef](#)]
49. Wang, Y.; Qian, P.-Y. Conservative Fragments in Bacterial 16S rRNA Genes and Primer Design for 16S Ribosomal DNA Amplicons in Metagenomic Studies. *PLoS ONE* **2009**, *4*, e7401. [[CrossRef](#)] [[PubMed](#)]
50. de Figueiredo, D.R.; Lopes, A.R.; Pereira, M.J.; Polónia, A.R.; Castro, B.B.; Gonçalves, F.; Gomes, N.C.M.; Cleary, D.F.R. Bacterioplankton Community Shifts during a Spring Bloom of *Aphanizomenon gracile* and *Sphaerospermopsis aphanizomenoides* at a Temperate Shallow Lake. *Hydrobiology* **2022**, *1*, 499–517. [[CrossRef](#)]
51. Polónia, A.R.M.; Cleary, D.F.R.; Duarte, L.N.; de Voogd, N.J.; Gomes, N.C.M. Composition of Archaea in Seawater, Sediment, and Sponges in the Kepulauan Seribu Reef System, Indonesia. *Microb. Ecol.* **2014**, *67*, 553–567. [[CrossRef](#)] [[PubMed](#)]
52. Cleary, D.F.R.; Becking, L.E.; de Voogd, N.J.; Pires, A.C.C.; Polónia, A.R.M.; Egas, C.; Gomes, N.C.M. Habitat- and Host-Related Variation in Sponge Bacterial Symbiont Communities in Indonesian Waters. *FEMS Microbiol. Ecol.* **2013**, *85*, 465–482. [[CrossRef](#)] [[PubMed](#)]
53. de Voogd, N.J.; Cleary, D.F.R.; Polónia, A.R.M.; Gomes, N.C.M. Bacterial Community Composition and Predicted Functional Ecology of Sponges, Sediment and Seawater from the Thousand Islands Reef Complex, West Java, Indonesia. *FEMS Microbiol. Ecol.* **2015**, *91*, fiv019. [[CrossRef](#)] [[PubMed](#)]
54. Cleary, D.F.R.; de Voogd, N.J.; Polónia, A.R.M.; Freitas, R.; Gomes, N.C.M. Composition and Predictive Functional Analysis of Bacterial Communities in Seawater, Sediment and Sponges in the Spermonde Archipelago, Indonesia. *Microb. Ecol.* **2015**, *70*, 889–903. [[CrossRef](#)]
55. Edgar, R.C. UPARSE: Highly Accurate OTU Sequences from Microbial Amplicon Reads. *Nat. Methods* **2013**, *10*, 996–998. [[CrossRef](#)] [[PubMed](#)]
56. Edgar, R.C.; Haas, B.J.; Clemente, J.C.; Quince, C.; Knight, R. UCHIME Improves Sensitivity and Speed of Chimera Detection. *Bioinformatics* **2011**, *27*, 2194–2200. [[CrossRef](#)] [[PubMed](#)]
57. Zhang, Z.; Schwartz, S.; Wagner, L.; Miller, W. A Greedy Algorithm for Aligning DNA Sequences. *J. Comput. Biol.* **2000**, *7*, 203–214. [[CrossRef](#)] [[PubMed](#)]
58. R Core Team. *R: A Language and Environment for Statistical Computing*; R Foundation for Statistical Computing: Vienna, Austria, 2013; ISBN 3-900051-07-0.
59. Borcard, D.; Legendre, P. All-Scale Spatial Analysis of Ecological Data by Means of Principal Coordinates of Neighbour Matrices. *Ecol. Model.* **2002**, *153*, 51–68. [[CrossRef](#)]
60. Dray, S.; Legendre, P.; Peres-Neto, P.R. Spatial Modelling: A Comprehensive Framework for Principal Coordinate Analysis of Neighbour Matrices (PCNM). *Ecol. Model.* **2006**, *196*, 483–493. [[CrossRef](#)]
61. Oksanen, J.; Kindt, R.; Legendre, P.; O'Hara, B.; Simpson, G.L.; Solymos, P.; Henry, M.; Stevens, H.H.W. *Vegan: Community Ecology Package*; R Package Version 1.15-2; The R Project for Statistical Computing: Vienna, Austria, 2009.
62. Legendre, P.; Gallagher, E.D. Ecologically Meaningful Transformations for Ordination of Species Data. *Oecologia* **2001**, *129*, 271–280. [[CrossRef](#)]
63. Makarek, V.; Legendre, P. Nonlinear Redundancy Analysis and Canonical Correspondence Analysis Based on Polynomial Regression. *Ecology* **2002**, *83*, 1146–1161. [[CrossRef](#)]
64. Cleary, D.F.R.; Becking, L.E.; De Voogd, N.J.; Renema, W.; De Beer, M.; Van Soest, R.W.M.; Hoeksema, B.W. Variation in the Diversity and Composition of Benthic Taxa as a Function of Distance Offshore, Depth and Exposure in the Spermonde Archipelago, Indonesia. *Estuar. Coast. Shelf Sci.* **2005**, *65*, 557–570. [[CrossRef](#)]
65. Ohmann, J.L.; Spies, T.A. Regional Gradient Analysis and Spatial Pattern of Woody Plant Communities of Oregon Forests. *Ecol. Monogr.* **1998**, *68*, 151. [[CrossRef](#)]
66. Cleary, D.F.R.; Mooers, A.Ø.; Eichhorn, K.A.O.; Van Tol, J.; De Jong, R.; Menken, S.B.J. Diversity and Community Composition of Butterflies and Odonates in an ENSO-induced Fire Affected Habitat Mosaic: A Case Study from East Kalimantan, Indonesia. *Oikos* **2004**, *105*, 426–448. [[CrossRef](#)]
67. USEPA. *National Primary Drinking Water Regulations*; United States Environmental Protection Agency: Washington, DC, USA, 2017.
68. Rakib, M.A.; Sasaki, J.; Matsuda, H.; Quraishi, S.B.; Mahmud, M.J.; Bodrud-Doza, M.; Ullah, A.K.M.A.; Fatema, K.J.; Newaz, M.A.; Bhuiyan, M.A.H. Groundwater Salinization and Associated Co-Contamination Risk Increase Severe Drinking Water Vulnerabilities in the Southwestern Coast of Bangladesh. *Chemosphere* **2020**, *246*, 125646. [[CrossRef](#)]

69. Tiwari, A.K.; Pisciotta, A.; De Maio, M. Evaluation of Groundwater Salinization and Pollution Level on Favignana Island, Italy. *Environ. Pollut.* **2019**, *249*, 969–981. [\[CrossRef\]](#)
70. Carreira, P.M.; Bahir, M.; Salah, O.; Galego Fernandes, P.; Nunes, D. Tracing Salinization Processes in Coastal Aquifers Using an Isotopic and Geochemical Approach: Comparative Studies in Western Morocco and Southwest Portugal. *Hydrogeol. J.* **2018**, *26*, 2595–2615. [\[CrossRef\]](#)
71. Carreira, P.M.; Marques, J.M.; Nunes, D. Source of Groundwater Salinity in Coastline Aquifers Based on Environmental Isotopes (Portugal): Natural vs. Human Interference. A Review and Reinterpretation. *Appl. Geochem.* **2014**, *41*, 163–175. [\[CrossRef\]](#)
72. Marques, A.C.; Carvalho, R.; da Silva, E.F. Salinization as Groundwater Contamination in Estarreja Shallow Aquifer, Aveiro (Portugal). In *Advances in Geoethics and Groundwater Management: Theory and Practice for a Sustainable Development*; Advances in Science, Technology & Innovation; Springer: Cham, Switzerland, 2021. [\[CrossRef\]](#)
73. Cruz, J.V.; Andrade, C. Groundwater Salinization in Graciosa and Pico Islands (Azores Archipelago, Portugal): Processes and Impacts. *J. Hydrol. Reg. Stud.* **2017**, *12*, 69–87. [\[CrossRef\]](#)
74. Song, Y.; Mao, G.; Gao, G.; Bartlam, M.; Wang, Y. Structural and Functional Changes of Groundwater Bacterial Community During Temperature and PH Disturbances. *Microb. Ecol.* **2019**, *78*, 428–445. [\[CrossRef\]](#)
75. Chae, G.T.; Kim, K.; Yun, S.T.; Kim, K.H.; Kim, S.O.; Choi, B.Y.; Kim, H.S.; Rhee, C.W. Hydrogeochemistry of Alluvial Groundwaters in an Agricultural Area: An Implication for Groundwater Contamination Susceptibility. *Chemosphere* **2004**, *55*, 369–378. [\[CrossRef\]](#)
76. Leyden, E.; Cook, F.; Hamilton, B.; Zammit, B.; Barnett, L.; Lush, A.M.; Stone, D.; Mosley, L. Near Shore Groundwater Acidification during and after a Hydrological Drought in the Lower Lakes, South Australia. *J. Contam. Hydrol.* **2016**, *189*, 44–57. [\[CrossRef\]](#)
77. Franken, G.; Postma, D.; Duijnisveld, W.H.M.; Böttcher, J.; Molson, J. Acid Groundwater in an Anoxic Aquifer: Reactive Transport Modelling of Buffering Processes. *Appl. Geochem.* **2009**, *24*, 890–899. [\[CrossRef\]](#)
78. Sena, C.; Teresa Condesso de Melo, M. Groundwater-Surface Water Interactions in a Freshwater Lagoon Vulnerable to Anthropogenic Pressures (Pateira de Fermentelos, Portugal). *J. Hydrol.* **2012**, *466–467*, 88–102. [\[CrossRef\]](#)
79. Lasagna, M.; De Luca, D.A.; Franchino, E. Nitrate Contamination of Groundwater in the Western Po Plain (Italy): The Effects of Groundwater and Surface Water Interactions. *Environ. Earth Sci.* **2016**, *75*, 240. [\[CrossRef\]](#)
80. Mueller, Y.K.; Goldscheider, N.; Eiche, E.; Emberger, H.; Goepfert, N. From Cave to Spring: Understanding Transport of Suspended Sediment Particles in a Fully Phreatic Karst Conduit Using Particle Analysis and Geochemical Methods. *Hydrol. Process* **2023**, *37*, e14979. [\[CrossRef\]](#)
81. Hose, G.C.; Di Lorenzo, T.; Fillinger, L.; Galassi, D.M.P.; Griebler, C.; Hahn, H.J.; Handley, K.M.; Korbel, K.; Reboleira, A.S.P.S.; Siemensmeyer, T.; et al. Assessing groundwater ecosystem health, status and services. In *Groundwater Ecology and Evolution*; Malard, F., Griebler, C., Rétaux, S., Eds.; Academic Press: Cambridge, MA, USA, 2023; pp. 501–524. [\[CrossRef\]](#)
82. Sagova-Mareckova, M.; Boenigk, J.; Bouchez, A.; Cermakova, K.; Chonova, T.; Cordier, T.; Eisendle, U.; Elersek, T.; Fazi, S.; Fleituch, T.; et al. Expanding Ecological Assessment by Integrating Microorganisms into Routine Freshwater Biomonitoring. *Water Res.* **2021**, *191*, 116767. [\[CrossRef\]](#) [\[PubMed\]](#)
83. de Figueiredo, D.R.; Ferreira, R.V.; Cerqueira, M.; de Melo, T.C.; Pereira, M.J.; Castro, B.B.; Correia, A. Impact of Water Quality on Bacterioplankton Assemblage along Cértima River Basin (Central Western Portugal) Assessed by PCR–DGGE and Multivariate Analysis. *Environ. Monit. Assess.* **2012**, *184*, 471–485. [\[CrossRef\]](#) [\[PubMed\]](#)
84. de Figueiredo, D.R.; Pereira, M.J.; Moura, A.; Silva, L.; Bárrios, S.; Fonseca, F.; Henriques, I.; Correia, A. Bacterial Community Composition over a Dry Winter in Meso- and Eutrophic Portuguese Water Bodies. *FEMS Microbiol. Ecol.* **2007**, *59*, 638–650. [\[CrossRef\]](#)
85. de Figueiredo, D.R.; Pereira, M.J.; Castro, B.B.; Correia, A. Bacterioplankton Community Composition in Portuguese Water Bodies under a Severe Summer Drought. *Community Ecol.* **2012**, *13*, 185–193. [\[CrossRef\]](#)
86. Osburn, M.R.; Selensky, M.J.; Beddows, P.A.; Jacobson, A.; DeFranco, K.; Merediz-Alonso, G. Microbial Biogeography of the Eastern Yucatán Carbonate Aquifer. *Appl. Environ. Microbiol.* **2023**, *89*, e0168223. [\[CrossRef\]](#)
87. Barnett, M.J.; Farr, G.J.; Shen, J.; Gregory, S. Groundwater Microbiology of an Urban Open-Loop Ground Source Heat Pump with High Methane. *Groundwater* **2023**, *61*, 274–287. [\[CrossRef\]](#)
88. Chen, X.; Ye, Q.; Du, J.; Cukrov, N.; Cukrov, N.; Zhang, Y.; Li, L.; Zhang, J. Linking Bacterial and Archaeal Community Dynamics to Related Hydrological, Geochemical and Environmental Characteristics between Surface Water and Groundwater in a Karstic Estuary. *Acta Oceanol. Sin.* **2023**, *42*, 158–170. [\[CrossRef\]](#)
89. Visser, A.N.; Martin, J.D.; Osenbrück, K.; Rügner, H.; Grathwohl, P.; Kappler, A. In Situ Incubation of Iron(II)-Bearing Minerals and Fe(0) Reveals Insights into Metabolic Flexibility of Chemolithotrophic Bacteria in a Nitrate Polluted Karst Aquifer. *Sci. Total Environ.* **2024**, *926*, 172062. [\[CrossRef\]](#)
90. Wu, M.; Lai, C.Y.; Wang, Y.; Yuan, Z.; Guo, J. Microbial Nitrate Reduction in Propane- or Butane-Based Membrane Biofilm Reactors under Oxygen-Limiting Conditions. *Water Res.* **2023**, *235*, 119887. [\[CrossRef\]](#)
91. Beganskas, S.; Gorski, G.; Weathers, T.; Fisher, A.T.; Schmidt, C.; Saltikov, C.; Redford, K.; Stoneburner, B.; Harmon, R.; Weir, W. A Horizontal Permeable Reactive Barrier Stimulates Nitrate Removal and Shifts Microbial Ecology during Rapid Infiltration for Managed Recharge. *Water Res.* **2018**, *144*, 274–284. [\[CrossRef\]](#)
92. Xia, Z.; Liu, G.; She, Z.; Gao, M.; Zhao, Y.; Guo, L.; Jin, C. Performance and Bacterial Communities in Unsaturated and Saturated Zones of a Vertical-Flow Constructed Wetland with Continuous-Feed. *Bioresour. Technol.* **2020**, *315*, 123859. [\[CrossRef\]](#)



93. Wang, H.; Li, P.; Liu, H.; Tan, T.; Yang, G.; Zhang, R. Microorganisms for Ammonia/Ammonium-Oxidization and Anammox in High Arsenic Holocene-Pleistocene Aquifers. *Int. Biodeterior. Biodegrad.* **2021**, *157*, 105136. [\[CrossRef\]](#)
94. Maharjan, A.K.; Kamei, T.; Amatya, I.M.; Mori, K.; Kazama, F.; Toyama, T. Ammonium-Nitrogen (NH<sub>4</sub><sup>+</sup>-N) Removal from Groundwater by a Dropping Nitrification Reactor: Characterization of NH<sub>4</sub><sup>+</sup>-N Transformation and Bacterial Community in the Reactor. *Water* **2020**, *12*, 599. [\[CrossRef\]](#)
95. Tatari, K.; Musovic, S.; Gülay, A.; Dechesne, A.; Albrechtsen, H.J.; Smets, B.F. Density and Distribution of Nitrifying Guilds in Rapid Sand Filters for Drinking Water Production: Dominance of *Nitrospira* spp. *Water Res.* **2017**, *127*, 239–248. [\[CrossRef\]](#)
96. Van de Graaf, A.A.; Mulder, A.; De Bruijn, P.; Jetten, M.S.M.; Robertson, L.A.; Kuenen, J.G. Anaerobic Oxidation of Ammonium Is a Biologically Mediated Process. *Appl. Environ. Microbiol.* **1995**, *61*, 1246–1251. [\[CrossRef\]](#)
97. Rivett, M.O.; Buss, S.R.; Morgan, P.; Smith, J.W.N.; Bemment, C.D. Nitrate Attenuation in Groundwater: A Review of Biogeochemical Controlling Processes. *Water Res.* **2008**, *42*, 4215–4232. [\[CrossRef\]](#) [\[PubMed\]](#)
98. Hu, J.; Zhao, Y.; Yang, W.; Wang, J.; Liu, H.; Zheng, P.; Hu, B. Surface Ammonium Loading Rate Shifts Ammonia-Oxidizing Communities in Surface Water-Fed Rapid Sand Filters. *FEMS Microbiol. Ecol.* **2020**, *96*, fiae179. [\[CrossRef\]](#) [\[PubMed\]](#)
99. Dangeti, S.; McBeth, J.M.; Roshani, B.; Vyskocil, J.M.; Rindall, B.; Chang, W. Microbial Communities and Biogenic Mn-Oxides in an on-Site Biofiltration System for Cold Fe(II)- and Mn(II)-Rich Groundwater Treatment. *Sci. Total Environ.* **2020**, *710*, 136386. [\[CrossRef\]](#)
100. Du, X.; Liu, G.; Qu, F.; Li, K.; Shao, S.; Li, G.; Liang, H. Removal of Iron, Manganese and Ammonia from Groundwater Using a PAC-MBR System: The Anti-Pollution Ability, Microbial Population and Membrane Fouling. *Desalination* **2017**, *403*, 97–106. [\[CrossRef\]](#)
101. Nitzsche, K.S.; Weigold, P.; Lösekann-Behrens, T.; Kappler, A.; Behrens, S. Microbial Community Composition of a Household Sand Filter Used for Arsenic, Iron, and Manganese Removal from Groundwater in Vietnam. *Chemosphere* **2015**, *138*, 47–59. [\[CrossRef\]](#)
102. Li, X.K.; Chu, Z.R.; Liu, Y.J.; Zhu, M.T.; Yang, L.; Zhang, J. Molecular Characterization of Microbial Populations in Full-Scale Biofilters Treating Iron, Manganese and Ammonia Containing Groundwater in Harbin, China. *Bioresour. Technol.* **2013**, *147*, 234–239. [\[CrossRef\]](#)
103. Vargha, M.; Róka, E.; Erdélyi, N.; Németh, K.; Nagy-Kovács, Z.; Kós, P.B.; Engloner, A.I. From Source to Tap: Tracking Microbial Diversity in a Riverbank Filtration-Based Drinking Water Supply System under Changing Hydrological Regimes. *Diversity* **2023**, *15*, 621. [\[CrossRef\]](#)
104. Herrmann, M.; Opitz, S.; Harzer, R.; Totsche, K.; Küsel, K. Attached and Suspended Denitrifier Communities in Pristine Limestone Aquifers Harbor High Fractions of Potential Autotrophs Oxidizing Reduced Iron and Sulfur Compounds. *Microb. Ecol.* **2017**, *74*, 264–277. [\[CrossRef\]](#) [\[PubMed\]](#)
105. Kumar, S.; Herrmann, M.; Blohm, A.; Hilke, I.; Frosch, T.; Trumbore, S.E.; Küsel, K. Thiosulfate- and Hydrogen-Driven Autotrophic Denitrification by a Microbial Consortium Enriched from Groundwater of an Oligotrophic Limestone Aquifer. *FEMS Microbiol. Ecol.* **2018**, *94*, fiy141. [\[CrossRef\]](#) [\[PubMed\]](#)
106. Kumar, S.; Herrmann, M.; Thamdrup, B.; Schwab, V.F.; Geesink, P.; Trumbore, S.E.; Totsche, K.U.; Küsel, K. Nitrogen Loss from Pristine Carbonate-Rock Aquifers of the Hainich Critical Zone Exploratory (Germany) Is Primarily Driven by Chemolithoautotrophic Anammox Processes. *Front. Microbiol.* **2017**, *8*, 1951. [\[CrossRef\]](#) [\[PubMed\]](#)
107. Chakraborty, A.; Suchy, M.; Hubert, C.R.J.; Ryan, M.C. Vertical Stratification of Microbial Communities and Isotope Geochemistry Tie Groundwater Denitrification to Sampling Location within a Nitrate-Contaminated Aquifer. *Sci. Total Environ.* **2022**, *820*, 153092. [\[CrossRef\]](#) [\[PubMed\]](#)
108. Zeng, X.; Hosono, T.; Ohta, H.; Niidome, T.; Shimada, J.; Morimura, S. Comparison of Microbial Communities inside and Outside of a Denitrification Hotspot in Confined Groundwater. *Int. Biodeterior. Biodegrad.* **2016**, *114*, 104–109. [\[CrossRef\]](#)
109. Kojima, H.; Fukui, M. Sulfuritalea Hydrogenivorans Gen. Nov., Sp. Nov., a Facultative Autotroph Isolated from a Freshwater Lake. *Int. J. Syst. Evol. Microbiol.* **2011**, *61*, 1651–1655. [\[CrossRef\]](#)
110. Lu, S.; Yang, Y.; Yin, H.; Su, X.; Yu, K.; Sun, C. Microbial Community Structure of Arsenic-Bearing Groundwater Environment in the Riverbank Filtration Zone. *Water* **2022**, *14*, 1548. [\[CrossRef\]](#)
111. Tian, G.; Kong, Z.; Zhang, Y.; Qiu, L.; Wang, H.; Yan, Q. Simultaneous Ammonia and Nitrate Removal by Novel Integrated Partial Denitrification-Anaerobic Ammonium Oxidation-Bioelectrochemical System. *Bioresour. Technol.* **2024**, *396*, 130428. [\[CrossRef\]](#)
112. Ma, J.; Liu, H.; Dang, H.; Wu, X.; Yan, Y.; Zeng, T.; Li, W.; Chen, Y. Realization of Nitrite Accumulation in an Autotrophic-Heterotrophic Denitrification System Using Different S/N/C Ratios Coupled with ANAMMOX to Achieve Nitrogen Removal. *J. Chem. Technol. Biotechnol.* **2023**, *98*, 269–281. [\[CrossRef\]](#)
113. Ke, T.; Zhang, D.; Guo, H.; Xiu, W.; Zhao, Y. Geogenic Arsenic and Arsenotrophic Microbiome in Groundwater from the Hetao Basin. *Sci. Total Environ.* **2022**, *852*, 158549. [\[CrossRef\]](#)
114. Smith, R.J.; Jeffries, T.C.; Roudnew, B.; Fitch, A.J.; Seymour, J.R.; Delpin, M.W.; Newton, K.; Brown, M.H.; Mitchell, J.G. Metagenomic Comparison of Microbial Communities Inhabiting Confined and Unconfined Aquifer Ecosystems. *Environ. Microbiol.* **2012**, *14*, 240–253. [\[CrossRef\]](#)
115. Suhadolnik, M.L.S.; Salgado, A.P.C.; Scholte, L.L.S.; Bleicher, L.; Costa, P.S.; Reis, M.P.; Dias, M.F.; Ávila, M.P.; Barbosa, F.A.R.; Chartone-Souza, E.; et al. Novel Arsenic-Transforming Bacteria and the Diversity of Their Arsenic-Related Genes and Enzymes Arising from Arsenic-Polluted Freshwater Sediment. *Sci. Rep.* **2017**, *7*, 11231. [\[CrossRef\]](#)



116. Saha, A.; Gupta, A.; Sar, P. Metagenome Based Analysis of Groundwater from Arsenic Contaminated Sites of West Bengal Revealed Community Diversity and Their Metabolic Potential. *J. Environ. Sci. Health A Tox Hazard. Subst. Environ. Eng.* **2023**, *58*, 91–106. [\[CrossRef\]](#)
117. Wang, Y.; Li, P.; Jiang, Z.; Sinkkonen, A.; Wang, S.; Tu, J.; Wei, D.; Dong, H.; Wang, Y. Microbial Community of High Arsenic Groundwater in Agricultural Irrigation Area of Hetao Plain, Inner Mongolia. *Front. Microbiol.* **2016**, *7*, 1917. [\[CrossRef\]](#)
118. Diba, F.; Hoque, M.N.; Rahman, M.S.; Haque, F.; Rahman, K.M.J.; Moniruzzaman, M.; Khan, M.; Hossain, M.A.; Sultana, M. Metagenomic and Culture-Dependent Approaches Unveil Active Microbial Community and Novel Functional Genes Involved in Arsenic Mobilization and Detoxification in Groundwater. *BMC Microbiol.* **2023**, *23*, 241. [\[CrossRef\]](#)
119. Liu, Y.; Wan, Y.; Ma, Z.; Dong, W.; Su, X.; Shen, X.; Yi, X.; Chen, Y. Effects of Magnetite on Microbially Driven Nitrate Reduction Processes in Groundwater. *Sci. Total Environ.* **2023**, *855*, 158956. [\[CrossRef\]](#)
120. Kanarek, P.; Bogiel, T.; Breza-Boruta, B. Legionellosis Risk—An Overview of *Legionella* spp. *Habitats Eur. Environ. Sci. Pollut. Res.* **2022**, *29*, 76532–76542. [\[CrossRef\]](#)
121. Sang, S.; Zhang, X.; Dai, H.; Hu, B.X.; Ou, H.; Sun, L. Diversity and Predictive Metabolic Pathways of the Prokaryotic Microbial Community along a Groundwater Salinity Gradient of the Pearl River Delta, China. *Sci. Rep.* **2018**, *8*, 17317. [\[CrossRef\]](#)
122. Mohr, K.I. Diversity of Myxobacteria—We Only See the Tip of the Iceberg. *Microorganisms* **2018**, *6*, 84. [\[CrossRef\]](#)
123. Zhang, Y.; Kelly, W.R.; Panno, S.V.; Liu, W.-T. Tracing Fecal Pollution Sources in Karst Groundwater by Bacteroidales Genetic Biomarkers, Bacterial Indicators, and Environmental Variables. *Sci. Total Environ.* **2014**, *490*, 1082–1090. [\[CrossRef\]](#)
124. Stegen, J.C.; Fredrickson, J.K.; Wilkins, M.J.; Konopka, A.E.; Nelson, W.C.; Arntzen, E.V.; Chrisler, W.B.; Chu, R.K.; Danczak, R.E.; Fansler, S.J.; et al. Groundwater-Surface Water Mixing Shifts Ecological Assembly Processes and Stimulates Organic Carbon Turnover. *Nat. Commun.* **2016**, *7*, 11237. [\[CrossRef\]](#)
125. Kwon, M.J.; Yun, S.T.; Ham, B.; Lee, J.H.; Oh, J.S.; Jheong, W.W. Impacts of Leachates from Livestock Carcass Burial and Manure Heap Sites on Groundwater Geochemistry and Microbial Community Structure. *PLoS ONE* **2017**, *12*, e0182579. [\[CrossRef\]](#)

**Disclaimer/Publisher’s Note:** The statements, opinions and data contained in all publications are solely those of the individual author(s) and contributor(s) and not of MDPI and/or the editor(s). MDPI and/or the editor(s) disclaim responsibility for any injury to people or property resulting from any ideas, methods, instructions or products referred to in the content.